

RESEARCH

Open Access



Upcycling depolymerized PET waste into polyhydroxyalkanoates and triacylglycerols by a newly isolated *Rhodococcus* sp. strain

Ana Teresa Rebocho^{1,2}, Cristiana A. V. Torres^{1,2*}, Helena Koninckx³, Lutgart Stragier³, Olivia A. Attallah⁴, Marija Mojicevic⁴, Cuneyt Erdinc Tas⁴, Margaret Brennan Fournet⁴, Maria A. Reis^{1,2} and Filomena Freitas^{1,2}

Abstract

The use of post-consumer polyethylene terephthalate (PET) wastes, which often contain various additives and contaminants such as metals and pigments that make mechanical recycling and reusability difficult, as feedstocks for microbial synthesis of value-added bio-based products is an emerging sustainable strategy for managing such wastes. This study evaluated the ability of a strain isolated from a plastic-contaminated site, *Rhodococcus* sp. isolate Ave7, to use terephthalic acid (TPA) obtained by chemically depolymerizing PET waste, as sole feedstock for cell growth and production of polyhydroxyalkanoates (PHAs) and triacylglycerols (TAGs) as intracellular storage compounds. The fed-batch bioreactor cultivation resulted in a cell dry weight production of 3.85 g/L, with PHA and TAG contents of 15.0 wt.% and 15.4 wt.%, respectively. Overall, the culture consumed 16.5 g/L TPA over a period of 73 h. The produced PHA was mainly composed of 3-hydroxyvalerate (3HV) monomers (> 90 wt.%). The accumulated TAGs presented a fatty acids profile rich in octadecenoic acid (C_{18:1}; 52 wt.%), hexadecanoic acid (C_{16:0}; 32 wt.%) and octadecanoic acid (C_{18:0}; 12 wt.%). Overall, the strain *Rhodococcus* sp. Ave7 demonstrated a high capacity for TPA removal, converting it into cell biomass, PHA and TAGs, thus rendering this bioprocess a promising solution to reduce the plastic waste burden, in a circular and sustainable approach.

Keywords Plastic upcycling, Biodegradation, *Rhodococcus*, Polyethylene terephthalate, Polyhydroxyalkanoates, Poly(3-hydroxybutyrate-co-3-hydroxyvalerate), Triacylglycerols

Introduction

Polyethylene terephthalate (PET) is a widely used thermoplastic, synthesized through the condensation of terephthalic acid (TPA) and ethylene glycol (EG) [1]. Given

its simple synthesis, low-cost production, thermostability and durability, make it extensively used in packaging industries, namely plastic bottles of soft drinks, food jars, clothing, and plastic films [2, 3]. Despite accounting for 6.2% of the worldwide plastics' production, only 25% of PET is recycled in Europe, with the majority discarded in the environment [4, 5].

The increasing demand and inadequate disposal of PET have led to severe environmental pollution, as large volumes escape proper waste management systems, contaminating oceans and ecosystems. Due to its resistance to microbial degradation, PET persists for centuries, intensifying plastic waste accumulation [6, 7]. Managing PET waste remains a critical challenge, as conventional

*Correspondence:

Cristiana A. V. Torres
c.torres@fct.unl.pt

¹ i4HB - Institute for Health and Bioeconomy, NOVA School of Science and Technology, NOVA University Lisbon, Caparica 2829-516, Portugal

² UCIBIO - Applied Molecular Biosciences Unit, Department of Chemistry, NOVA School of Science and Technology, NOVA University Lisbon, Caparica 2829-516, Portugal

³ Avecom NV, Industrieweg 122P, Wondelgem 9032, Belgium

⁴ LIFE Research Institute, Technological University of the Shannon Midlands Midwest, Athlone N37 HD68, Ireland



© The Author(s) 2025. **Open Access** This article is licensed under a Creative Commons Attribution-NonCommercial-NoDerivatives 4.0 International License, which permits any non-commercial use, sharing, distribution and reproduction in any medium or format, as long as you give appropriate credit to the original author(s) and the source, provide a link to the Creative Commons licence, and indicate if you modified the licensed material. You do not have permission under this licence to share adapted material derived from this article or parts of it. The images or other third party material in this article are included in the article's Creative Commons licence, unless indicated otherwise in a credit line to the material. If material is not included in the article's Creative Commons licence and your intended use is not permitted by statutory regulation or exceeds the permitted use, you will need to obtain permission directly from the copyright holder. To view a copy of this licence, visit <http://creativecommons.org/licenses/by-nc-nd/4.0/>.

disposal methods such as landfilling and incineration pose several disadvantages, including slow degradation rates in landfills, limited spaces, long-term risks of contamination of soils and groundwater with leachate containing toxic compounds (e.g. heavy metals, dioxins, furans and polychlorinated biphenyls), and the emission of greenhouse gases associated with incineration [2, 8].

Recycling is currently regarded as the most sustainable PET waste management strategy and is categorized into four types [9]. Primary recycling involves mechanical re-extrusion of clean and single-type PET into materials with similar properties [10], though it is limited by contamination and material degradation over multiple cycles [11]. Secondary recycling processes PET through cleaning, shredding and remelting into flakes or pellets, but it requires high water consumption to remove contaminants (e.g. polymers, dirt, and labels) and often results in downcycling due to thermal degradation [10, 12, 13]. Furthermore, tertiary recycling recovers monomers, oligomers or additives via chemical depolymerization methods such as hydrolysis, glycolysis, aminolysis and methanolysis [14, 15]. Although effective for heterogeneous PET waste streams, this process is costly, energy-intensive, susceptible to equipment corrosion, and generates waste solvents [16, 17]. Lastly, quaternary recovery harnesses PET's high calorific value through combustion, but it is often associated with the release of toxic fumes [18].

The complexity of PET waste, often mixed with municipal waste and containing multilayered plastics, rubber, aluminium and functional additives, that are designed for specific packaging functions, poses significant challenges to effective recycling [19]. To address these challenges, upcycling strategies combining depolymerization and bioconversion are being explored to enhance PET waste valorisation [20, 21]. PET depolymerization yields intermediates, such as TPA, which can serve as microbial substrates, suitable for bioconversion by TPA-metabolizing microorganisms via specific metabolic pathways [21]. This biological approach enables the transformation of PET waste into high-value products with diverse applications [22, 23]. Recent studies have confirmed the microbial metabolism of TPA, EG and other PET degradation products into compounds, such as polyhydroxyalkanoates (PHA) [24–28], hydroxyalkanoxy-alkanoates (HAAs) [27], bacterial cellulose [29], muconic acid [30], vanillic acid [31], β -keto adipic acid [32, 33], catechol, gallic acid and pyrogallol [33, 34].

Among microbial candidates for PET bioconversion, *Rhodococcus* has emerged as a promising genus due to their remarkable metabolic versatility and environmental resilience. Commonly found in contaminated sites, *Rhodococcus* species are known for degrading various recalcitrant compounds [35]. Several strains have been

identified for their ability to metabolize pollutants and convert complex substrates into valuable compounds via diverse catabolic pathways [36]. For example, *Rhodococcus jostii* RHA1 and *Rhodococcus* sp. SSM1 were reported to degrade TPA [37, 38], while *Rhodococcus* sp. DK17 and *R. erythropolis* PR4 can degrade aromatic and alicyclic rings, as well as alkanes, respectively [39]. Additionally, *R. aetherivorans* IAR1 was reported to convert toluene into PHA and triacylglycerols (TAGs) [40], while *R. erythropolis* MTCC3951 and *R. pyridinivorans* P23 exhibit both TPA degradation and PHA production capabilities [41, 42].

Furthermore, *Rhodococcus* sp. can synthesize other valuable compounds with environmental and industrial relevance, including biosurfactants and carotenoids [35], PHA [43], wax esters (WEs) and TAGs [44, 45]. Their metabolic versatility makes them strong candidates for bioconversion and bioremediation, with potential applications in breaking down persistent plastic pollutants like polyethylene [46] and producing sustainable bioproducts such as PHA and TAGs [47]. This aligns with circular economy principles, offering an eco-friendly alternative to traditional PET waste management [35].

In this study, *Rhodococcus* sp. isolate Ave7 was cultivated in bioreactor using chemically depolymerized post-consumer PET waste, with TPA as the sole carbon source. The strain's ability to produce intracellular reserves of PHA and TAGs was evaluated under different cultivation modes, including batch and fed-batch processes. Following cultivation, the bioproducts were extracted and characterized, including an analysis of their composition, as well as the molecular mass distribution and thermal properties for PHA.

Materials and methods

Feedstock processing and characterization

Chemical depolymerization of post-consumer PET waste

Post-consumer PET waste (Fig. 1(A)), containing approximately 2–5% polyethylene (PE), 1–2% pigments, metallic ingredients and carbon black additives, was supplied by Novelplast (Ireland). This material was used as the standard substrate without further processing. Depolymerization experiments via reactive extrusion (REX) were conducted using a bench-top Prism™ twin-screw extruder (Thermo Electron GmbH, Karlsruhe, Germany) following a modified procedure from Fournet et al. [48]. The PET waste feedstock was mixed with solid NaOH in a 2:1 (wt%/wt%) ratio. The well-mixed depolymerization reaction mixture was then dispensed through the main shaft into the barrel, which was maintained at a constant temperature of 250 °C, while the screw rotational speed was set at 20 rpm. The resulting REX product, named REX-PET, was subsequently processed to extract and



Fig. 1 Post-consumer PET waste (A), REX-PET chemical depolymerized sample obtained from reactive extrusion of post-consumer PET waste (B) and REX-TPA solution used for bioreactor cultivations (C)

separate its terephthalic acid (TPA) content, named reactive extrusion-terephthalic acid (REX-TPA) (Fig. 1(B)).

Characterization of depolymerized PET waste

The depolymerized PET waste was characterized in terms of particle size distribution, moisture and inorganic content, elemental analysis and FT-IR.

The particle size distribution of REX-PET was determined by sieving a sample (~100 g) in a mechanical sieving shaker, equipped with sieves of pore sizes ranging from 106 to 2000 μm . The sample was agitated for 10 min, and the material collected on each sieve was weighed separately to determine its respective fraction in the sample.

For the moisture content determination, REX-PET (~50 mg) was subjected to a temperature of 100 $^{\circ}\text{C}$ until a constant weight was achieved. Afterwards, the dried sample was placed at a temperature of 550 $^{\circ}\text{C}$ for 24 h, and the inorganic salts content was determined gravimetrically by weighing the resulting ashes. The elemental analysis of REX-PET was performed using an elemental analyzer (Thermo Finnigan-CE Instruments, Flash EA 1112 CHNS series, Italy). A REX-PET sample was characterized via Fourier-transform infrared spectroscopy (FT-IR) with a spectrum two spectrometer (Perkin-Elmer, Waltham, MA, USA) equipped with the attenuated total reflectance (ATR) accessory. The spectra were recovered based on eight scans between a resolution of 4000 and 400 cm^{-1} , at room temperature.

Depolymerized PET waste processing

For the bacterial cultivation experiments, REX-PET was processed into an aqueous solution (named REX-TPA), which was obtained by preparing a 3.33% (w/v) mixture of REX-PET (5 g) (Fig. 1(B)) in deionized water (150 mL), followed by homogenization at 600 rpm during 1 h. The mixture was filtered (using paper filters with pore

size 20 μm) followed by pH 7 normalization by HCl 5 M addition. The final solution contained approximately 20 mg/mL of REX-TPA, representing a recovery of 60% (Fig. 1(C)). The solution of REX-TPA was assessed for its pH, moisture and inorganic content, ICP, total carbon and TPA quantification.

Moisture and inorganic content were also determined for REX-TPA samples (~5 mL) as determined as described in the previous section. REX-TPA samples (~5 mL) were filtered (0.2 μm nylon, Whatman) and analysed by inductively coupled plasma-atomic emission spectrometry (ICP-AES) (Horiba Jobin-Yvon, France, Ultima, equipped with a 40.68 MHz RF generator, Czerny-Turner monochromator with 1.00 m (sequential) and autosampler AS500). The Total Carbon (TC) was analysed in a TOC-VCSH Analyser (Shimadzu) with a combustion catalytic oxidation at a temperature of 680 $^{\circ}\text{C}$. High purity air served as carrier gas at a flow rate of 150 mL/min. TPA concentration was determined by high performance liquid chromatography (HPLC) using an Agilent Eclipse C18 250 \times 4.6 mm, coupled to a UV detector. The analysis was performed at 50 $^{\circ}\text{C}$, with samples eluted in isocratic mode using methanol (Fisher Chemical, HPLC grade) and 0.1% formic acid (Sigma-Aldrich, HPLC grade) solution (1:1, v/v). The flow rate was set to 1 mL/min, and the injection volume 5 μL [49]. TPA detection was obtained at 240 nm. A TPA stock solution (1 g/L) (Merck Millipore, 98%) was prepared in a phosphate buffer (containing per liter: $(\text{NH}_4)_2\text{HPO}_4$, 1.1 g (PanReac AppliChem, 99%); K_2HPO_4 , 5.8 g (PanReac AppliChem, 99%); KH_2PO_4 , 3.7 g (ChemLab, 99.5%)) and adjusted to pH 7. From this stock solution, TPA standards were prepared by serial dilution with a water-methanol mixture (10% methanol, Fisher Chemical, HPLC grade) to achieve TPA concentrations ranging from 4 to 400 mg/L. Similarly, the cell-free supernatant samples were diluted in the same 10% methanol aqueous solution to ensure consistency of

the standards and samples matrix for the HPLC analysis. All measurements were done in triplicate.

Microorganism

Rhodococcus sp. Ave 7 was isolated from landfill soil, by serially diluting and cultivating a sample on selective plates, containing commercial TPA (Merck Millipore, 98%) as carbon source. Single colonies were isolated and used for the amplification of the 16S rRNA gene via colony PCR using a T100 Thermal Cycler (Bio-Rad). The amplified 16S rRNA genes were then sent to Macrogen Europe (The Netherlands) for Sanger sequencing.

Culture media

Mineral salt medium (MSM) containing 8.86 g/L K_2HPO_4 (PanReac AppliChem, 99%), 2.80 g/L KH_2PO_4 (ChemLab, 99.5%), 0.50 g/L NaCl (PanReac AppliChem, 99.5%), 0.10 g/L $MgSO_4 \cdot 7H_2O$ (Biochem Chemopharma, 99.5%) and 0.10 g/L NH_4Cl (Biochem Chemopharma, 99.5%), was used for all experiments. The micronutrients' solution was added to the medium at a concentration of 10 mL/L. The micronutrients solution contained the following (per liter): $FeSO_4 \cdot 7H_2O$, 1.83 g; $MnSO_4 \cdot 1H_2O$, 0.56 g; $ZnSO_4 \cdot 7H_2O$, 1.35 g; $CaCl_2 \cdot 2H_2O$, 0.067 g; $CoSO_4 \cdot 7H_2O$, 0.036 g; $CuSO_4 \cdot 5H_2O$, 0.036 g; H_3BO_3 , 0.65 g; EDTA disodium $\cdot 2H_2O$, 1.104 g. This medium was used for inocula preparation of all assays. The medium was supplemented with terephthalic acid (TPA) (Merck Millipore, 98%) as carbon source at a concentration of 0.5 g/L for inocula preparation. For bioreactor assays, MSM was supplemented with REX-TPA solution (prepared as described above), to achieve a final TPA concentration of 12 g/L. All media were sterilized by autoclaving at 121 °C and 1 bar, for 30 min.

Bioreactor cultivations

Three bioreactor experiments were performed under different modes of cultivation: batch (Assay A) and fed-batch with pulse feeding (Assay B) or continuous feeding (Assay C). The inocula for the bioreactor assays were prepared by inoculating 1 mL of the cryopreserved culture into 200 mL MSM, prepared as described above, in a 500 mL baffled shake flask. The flasks were incubated in a rotary shaker (200 rpm), at 30 °C, for 48 h. For the bioreactor assays, MSM supplemented with REX-TPA (12 g/L) and ammonia (0.3 g/L), yielding a C/N ratio of 29.7 (gC/gN), was prepared.

After sterilization in an autoclave at 121 °C, 1 bar, for 30 min, the medium was inoculated with 200 mL of the prepared bacterial culture to initiate the experiments.

Throughout the assays, the pH was monitored but not controlled. The temperature was controlled at 30 ± 0.1 °C in all assays. An aeration rate of 2 SLPM (standard liters

per minute) was kept during the experiments. The dissolved oxygen (DO) concentration was controlled at 20% of the air saturation, by automatically adjusting the stirring rate between 300 and 1000 rpm. Foam formation was automatically suppressed by addition of Antifoam 204 (Sigma-Aldrich).

Assay A, under batch mode, was conducted in a 3 L bioreactor (Jupiter 3, Solaris, Italy), with initial working volume of 2 L. Assay B was performed in a 5 L bioreactor (Jupiter 6.0, Solaris, Italy) with an initial working volume of 2 L. After initial TPA depletion, signalled by an abrupt increase of DO concentration, REX-TPA pulse (1 L) containing 20 g/L TPA was fed to the bioreactor. Assay C was performed in a 3 L bioreactor (Bionet F1, Spain), with an initial working volume of 1.5 L. A continuous feeding of a REX-TPA solution containing 20 g/L TPA and 0.01 g/L of ammonia, was fed to the bioreactor at a 0.1 L/h flow rate for 15 h.

Samples (10–20 mL) were periodically taken from the bioreactor for quantification of the cell dry weight (CDW), TPA, ammonium, PHA and TAG.

Analytical methods

CDW quantification

For determination of the CDW, culture broth samples (5 mL) were centrifuged (20 min at 18,516 g, 4 °C). The cell pellet was washed with deionized water (5 mL) twice and lyophilized for 48 h. The CDW was determined gravimetrically by weighing the dried cell pellets. All measurements were done in triplicate.

Quantification of TPA

TPA concentration was determined using HPLC, as described above, with an Agilent Eclipse C18 column (250 × 4.6 mm) and UV detection at 240 nm. The analysis was conducted at 50 °C in isocratic mode with a mobile phase of methanol and 0.1% formic acid (1:1, v/v), at a flow rate of 1 mL/min and an injection volume of 5 µL. A TPA stock solution (1 g/L) was prepared in phosphate buffer (pH 7), and TPA standards were prepared through serial dilution to obtain concentrations ranging from 4 to 400 mg/L. Cell-free supernatant samples were diluted with a 10% methanol–water solution to match the matrix of the standards. All measurements were performed in triplicate.

Ammonium quantification

Ammonia concentration was determined by colorimetry using a flow segmented analyser (Skalar 5100, Skalar Analytical, Netherlands). NH_4Cl (Biochem Chemopharma, 99.5%) samples at concentrations ranging from 2 to 20 mg/L were used as standards. All measurements were done in triplicate.

PHA and TAGs quantification

Storage compounds content in the biomass, namely PHA and TAGs, and their composition were determined by gas chromatography (GC) after acidic methanolysis of freeze-dried cells' samples. Freeze dried samples (3 to 5 mg) were mixed with 2 mL 20% (v/v) sulphuric acid (Honeywell Fluka, HPLC grade) in methanol (Fisher Chemical, HPLC grade) and 2 mL benzoic acid in chloroform (0.5 g/L) (Fisher Chemical, HPLC grade) and heated at 100 °C, for 4 h. Benzoic acid (Sigma-Aldrich, ≥ 99.5%) acted as internal standard. The calibration curve for PHA quantification was prepared using a standard solution of P(HB-co-HV) (Sigma-Aldrich) composed of 14 mol% 3-hydroxyvalerate (3HV). For TAGs quantification, a mixture of fatty acid methyl esters (FAME) composed of C₁₄-C₂₂ (Sigma-Aldrich) at concentrations ranging from 0.1 to 1.0 g/L was used. The methyl esters obtained from the methanolysis, derived simultaneously from both PHA and TAGs, were analysed in a single run using a Trace 1300 GC apparatus (Thermo Fisher Scientific, US) equipped with a flame ionization detector (FID) (Thermo Fisher Scientific, US) and a Restek column (Crossbond, Stabilwax). The system operated at constant pressure (96 kPa) using helium as carrier gas. The oven temperature program was the following: 20 °C/min until 100 °C; 3 °C/min until 155 °C and, finally, 20 °C/min until 230 °C with a holding time of 30 min. All measurements were done in triplicate.

Glycogen analysis

Glycogen accumulation was analysed following the protocol described by [50]. The previously weighed freeze-dried biomass was treated with 2 mL of a dilute solution of HCl. The tubes were incubated at 100 °C for 3 h. The samples were filtered (filter with 0.2 μm pore size, Whatman) and analysed by high-performance liquid chromatography (HPLC) using a chromatograph equipped with an Aminex HPX-87H HPLC column (Bio-Rad, USA). A solution of 0.01 N of H₂SO₄ was used as a mobile phase with a flow rate of 0.5 mL/min and a 30 °C operating temperature. The detection wavelength was set at 210 nm. Glucose (Scharlau, Barcelona, Spain) was used as standard ranging from 0.06 to 1 g/L. Samples were analysed in triplicate.

Polyphosphate staining method

For staining polyphosphate inclusions, samples were fixed with gentle heat on glass microscopic slides and exposed to Loeffler's methylene-blue staining in each case with light washing in distilled water [51].

Calculations

The maximum specific cell growth rate (μ_{max} , h⁻¹) was calculated by determining the linear regression slope of the exponential phase of $\ln X_t/X_0$ versus time curve, where X_t/X_0 (g/L) is the active cell biomass concentration at time t (h) and at the beginning of the run (t_0), respectively. The active cell biomass (X , g/L) (without PHA and TAG) used for yield calculations, at time t , was determined by Eq. (1).

$$X_t = CDW_t - (PHA_t + TAG_t) \quad (1)$$

where CDW_t (g/L), PHA_t (g/L) and TAG_t (g/L) represent the CDW and the concentrations of PHA and triacylglycerol (TAG) at time t (h), respectively.

The overall volumetric productivity (r_p , g/L.(day)), where P is indicative of PHA or TAG, were determined by Eq. (2):

$$r_p = \frac{\Delta P}{\Delta t} \quad (2)$$

where ΔP (g/L) is the product (PHA or TAG) produced in time interval Δt (h).

The yields of active biomass ($Y_{X/S}$, g_X/g_{TPA}) and the products (P) on substrate basis ($Y_{P/TPA}$, g_P/g_{TPA}) were determined by Eqs. (3) and (4):

$$Y_{X/S} = \frac{\Delta X}{\Delta S} \quad (3)$$

$$Y_{P/S} = \frac{\Delta P}{\Delta S} \quad (4)$$

where ΔX and ΔP are the active biomass and the PHA and/or TAG produced (g/L), respectively, and ΔS (g/L) is the concentration of TPA from REX-TPA residue consumed during the same time range of the cultivation run.

Statistical analysis

The statistical differences for the mean and standard deviation of the kinetic and stoichiometric parameters obtained from the three assays performed by *Rhodococcus* sp. Ave7 using REX-TPA were assessed using one-way ANOVA followed by Bonferroni's multiple comparison tests in GraphPad Prism 5 with the criteria for statistical significance set at $p < 0.05$.

Bioproducts extraction and characterization

The cultivation broth was centrifuged (10,350g, 20 min, 4 °C) and the obtained cell pellets were freeze-dried and milled. The bioproducts were extracted from the freeze-dried biomass by Soxhlet extraction with chloroform (Fisher Chemical, HPLC grade), at 80 °C, for 48 h. Later,

the PHA was precipitated in ice-cold ethanol (1:10, v/v), under vigorous stirring, and dried in a fume hood at room temperature [52].

The ethanol used for PHA precipitation was collected and allowed to evaporate at room temperature in a fume hood, to recover the produced TAGs.

For further purifying the PHA, the sample was mixed with 1-butanol ($\geq 99.5\%$, PanReac AppliChem) at a concentration of 0.3% (w/v), and heated to 75 °C for 2 h, under constant stirring, to dissolve the TAGs fraction. The solvent was removed while still hot and the insoluble PHA was recovered and left to dry at room temperature in a fume hood.

FT-IR

FT-IR analysis were conducted for the recovered TAGs and PHA samples in a Perkin-Elmer Spectrum two spectrometer coupled with ATR accessory. The polymer was directly analysed on the FTIR cells. The spectra were recorded between 400 and 4000 cm^{-1} resolution and 10 scans were conducted at room temperature.

Thermal properties

Differential scanning calorimetry (DSC) was carried out with a DSC Q2000 instrument (TA Instruments, New Castle, FL, USA). Hermetic aluminium pans were used to place the samples, and the analysis was performed with a heating and cooling rate of 10 °C/min over a temperature range of -90 °C to 180 °C, through three heating cycles. The endotherm peak's temperature and area of the first heating cycle were used to determine melting temperatures (T_m) and melting enthalpies (ΔH_m), respectively, while the glass transition temperature (T_g , °C) was taken as the midpoint of the heat flux step. The crystallinity (X_C , %) was estimated as the ratio between the obtained melting enthalpy and the melting enthalpy of 100% crystalline PHB, estimated as 146 J/g [53].

Thermogravimetric analysis (TGA) was performed using a thermogravimetric Analyzer Labsys EVO (Setaram, France), with weighing precision of $\pm 0.01\%$. Samples were placed in aluminium crucibles and analysed in argon atmosphere with temperature range between 25 and 800 °C, at a rate of 10 °C/min. The maximum thermal degradation temperature (T_{deg} , °C) corresponds to the temperature value obtained for the maximum decreasing peak of the sample mass.

Molecular mass distribution

Size-exclusion chromatography (SE-HPLC) was performed to determine the number average molecular weight (M_n), weight average molecular weight (M_w) and polydispersity index (M_w/M_n) of the PHA. Monodisperse polystyrene standards (370–2,520,000 Da) and the

biopolymer were prepared at a concentration of 0.2% (w/v) in chloroform. Analysis was conducted using a KNAUER Smartline SE-HPLC system (Berlin, Germany) equipped with a Phenomenex Phenogel Linear Liquid Chromatographic Column (300 \times 7.8 mm; Torrance, CA, USA), operated at 30 °C with a 1 mL/min chloroform flow rate as the mobile phase, using a Waters2414 refractive index detector (RID) (Milford, CT, USA).

Results and discussion

Feedstock characterization

The residue obtained from the depolymerization of PET waste, named REX-PET, was a uniform dark powder (Fig. 1(B)). The majority of the material comprised particles in the 1000–2000 μm size range ($46 \pm 2.0\%$ w/w), followed by particles larger than 2000 μm ($28 \pm 5.7\%$ w/w) and those at 500–1000 μm ($16 \pm 1.4\%$ w/w) (Fig. 2). Smaller particles (< 500 μm) collectively accounted for less than $12 \pm 1.1\%$ w/w. This particle size distribution indicates that the material is predominantly granular, with larger size fractions dominating the sample.

The moisture and inorganic content of REX-PET is shown in Table 1, and it presents a high inorganic salt content for REX-PET (46.46 ± 4.69 wt.%), since NaOH was used as a catalyst for the depolymerization of the PET waste, forming a sodium salt of TPA [54]. The elemental analysis (Table 1) revealed that REX-PET was mainly composed of carbon ($44.21 \pm 2.4\%$), with a minor hydrogen content ($2.97 \pm 0.39\%$) of trace of nitrogen ($0.04 \pm 0.02\%$), while no sulphur was detected.

As shown in Fig. 3, the spectral peaks of all REX-PET batches exhibited high similarity among the batch samples, although they differ from those reported for commercial TPA. The carboxylic group (-OH) stretching peak appears around 3000–2800 cm^{-1} , but it is less intense in the REX-PET samples, suggesting a lower concentration of free carboxylic acid groups compared to pure TPA [55]. The intense zone of peaks between 1718 and 1270 cm^{-1} correspond to the C=O and C=C bonds of the benzene ring in TPA, with intense peaks at 1557 and 1391 cm^{-1} indicative of the acidic carbonyl group (-C=O) and aromatic ring vibrations [55–57]. Notably, this region shows considerable differences from commercial TPA, as the peaks correspond to the formation of TPA disodium salt, a product of the depolymerization process [58]. This is evidenced by the absence of -O-H bending bond in REX-PET, at 940 cm^{-1} attributed to the presence of disodium terephthalate [59], and the disappearance of the carboxylic acid groups (-COOH) at 1625 and 1423 cm^{-1} [60]. Moreover, peaks displayed at 1088 and 1023 cm^{-1} can be attributed to the =C-H bending vibrations of the aromatic ring [56]. The FT-IR spectra of the three REX-PET samples in Fig. 3 show strong similarity among the

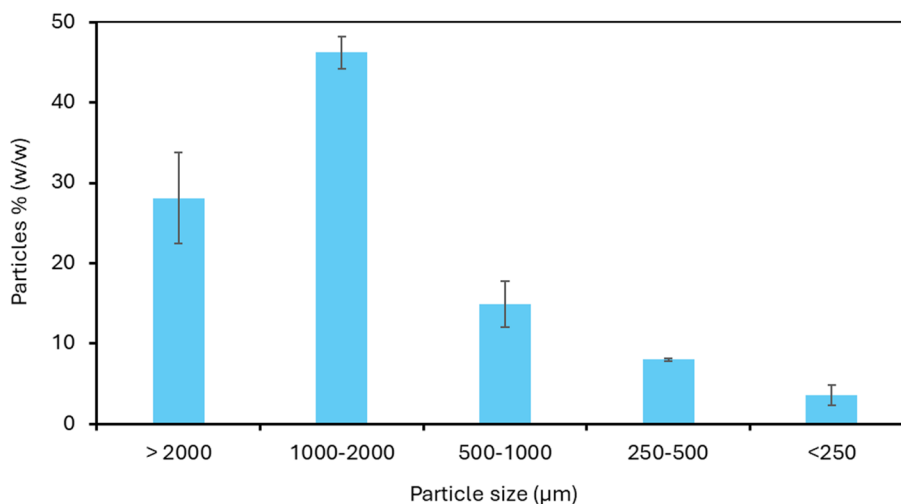


Fig. 2 Particle size distribution for REX-PET

Table 1 Characterization of REX-PET feedstock

| Parameter | REX-PET |
|-------------------------|--------------|
| Moisture (wt.%) | 1.07 ± 0.41 |
| Organic content (wt.%) | 52.47 ± 4.92 |
| Inorganic salts (wt.%) | 46.46 ± 4.69 |
| Elemental analysis (%): | |
| C | 44.21 ± 2.4 |
| H | 2.97 ± 0.39 |
| N | 0.04 ± 0.02 |
| S | n.d |

n.d. not detected

batches, indicating consistent chemical structures with no significant variations in peaks or intensities, reflecting a stable and reproducible depolymerization process.

The REX-TPA solution obtained from REX-PET presented a dark, translucent without visible suspended particles (after filtration) as can be observed in Fig. 1(C). The pH of the REX-TPA solution was found to be 11.05 (Table 2), which correlates with the dry REX depolymerization process that follows the hydrolysis method under alkaline conditions provided by adding NaOH [43]. This pH value is comparable to that obtained for a solution containing PET depolymerized upon reliable hydrolysis [61]. The REX-TPA solution had a total carbon (TC) content of 12.06 ± 0.24 g/L (as determined by the TOC-VCSH Analysis) and a TPA concentration of 19.69 ± 0.09 g/L (as determined by the HPLC analysis). This TPA concentration accounts for a carbon content of 11.39 g/L which shows that the solution predominantly comprised TPA, with only a minor content of other carbonaceous compounds.

The moisture and inorganic content (Table 2) for REX-TPA was of 96.20 ± 0.43 wt.% and 2.21 ± 0.13 wt.%, respectively. As expected, REX-TPA showed a high content in Na (461.12 ± 71.71 mg/L) (Table 2), which can be attributed to the depolymerization procedure conducted under alkaline conditions. Thus, HCl was used to neutralize the aqueous solution [62]. The main advantage of using this type of depolymerization conditions is its suitability for complex PET waste streams, which often contain significant amounts of metals, pigments or other types of plastic [9, 63]. Other elements found in REX-TPA were Fe (8.84 ± 2.45 mg/L), Ti (4.16 ± 1.48 mg/L), Sb (3.82 ± 1.23 mg/L), Si (2.12 ± 0.84 mg/L) and traces of Cr, Al, Zn, W and Mo (< 0.5 mg/L) (Table 2). This wide range of components found in REX-TPA reveals the high heterogeneity of additives that can be found in mixed plastic litter samples [64].

Batch bioreactor cultivation

Rhodococcus sp. Ave7 was cultivated under batch mode using an initial TPA concentration of 12 g/L as sole carbon source, under a controlled temperature of 30 °C and an initial pH of 7. The initial concentrations of TPA (12 g/L) and ammonium (0.3 g/L) in the bioreactor medium were determined based on prior findings from an RSM study (Table S1 and Fig. S1, Supplementary Material). This optimization study identified these parameters as most suitable for enhancing cell growth and the accumulation of intracellular storage compounds, namely PHA and TAGs.

After a 10-h lag phase, *Rhodococcus* sp. Ave7 entered an exponential phase, reaching a maximum specific cell growth rate of 0.18 ± 0.05 h⁻¹ and a CDW of 1.78 ± 0.08 g/L at 20 h of cultivation, when ammonia was exhausted

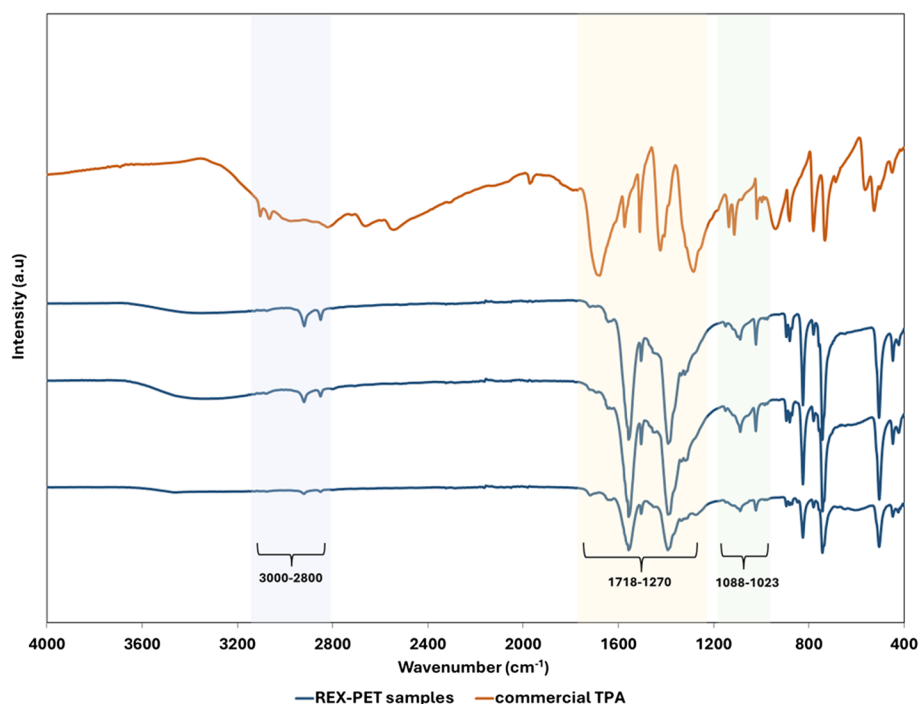


Fig. 3 Fourier-transform infrared (FT-IR) spectra of three batches of REX-PET samples derived from PET waste depolymerization under similar conditions, and of commercial TPA (Merck Millipore, 98%)

Table 2 Characterization of REX-TPA solution used in bioreactor media cultivation as feedstock

| Parameter | REX-TPA |
|------------------------|----------------|
| pH | 11.05 |
| Moisture (wt.%) | 96.20 ± 0.43 |
| Organic content (wt.%) | 1.58 ± 0.55 |
| Inorganic salts (wt.%) | 2.21 ± 0.13 |
| Total carbon (g/L) | 12.06 ± 0.24 |
| [TPA] (g/L) | 19.69 ± 0.09 |
| Element (mg/L) | |
| Na | 461.12 ± 71.71 |
| K | 9.30 ± 3.91 |
| Fe | 8.84 ± 2.45 |
| Ti | 4.16 ± 1.48 |
| Sb | 3.82 ± 1.23 |
| P | 3.74 ± 0.98 |
| Mg | 3.11 ± 0.86 |
| Ca | 2.15 ± 0.36 |
| Si | 2.12 ± 0.84 |
| Cr | 0.51 ± 0.28 |
| Cu | 0.29 ± 0.03 |
| Al | 0.27 ± 0.09 |
| Zn | 0.25 ± 0.18 |
| W | 0.25 ± 0.06 |
| Mo | 0.13 ± 0.06 |

(Fig. 4(A1)). A final CDW of 2.67 ± 0.06 g/L was reached at the end of the assay. This value is slightly higher than the 2.3 g/L of CDW reported for *Pseudomonas umsongensis* G016 KS3 grew in a batch reactor, with similar duration, using as carbon source TPA and EG monomers obtained by enzymatic PET hydrolysis [27].

PHA accumulation started during the exponential cell growth phase, at 13 h of cultivation, and continued (Fig. 4(A2)) until the end of the assay, reaching a maximum PHA content in the biomass of 4.22 ± 0.03 wt.%, corresponding to a PHA concentration of 0.11 ± 0.02 g/L (Table 3). Slightly higher values were reported for *P. umsongensis* G016 KS3 (7 wt.%), corresponding to 0.15 g/L of PHA [27].

TAGs synthesis was initiated later, at around 21 h of cultivation (Fig. 4(A2)), reaching an intracellular content of 13.45 ± 0.69 wt.% and a concentration of 0.15 g/L by 21 h of cultivation (Table 3). This corresponds to an overall volumetric productivity of 0.305 g/(L day). During the first 21 h, the bacterial strain consumed 7.74 g of TPA, for both cellular growth and PHA accumulation, resulting in growth yield of 0.19 g_X/g_{TPA}. After ammonium depletion, the culture used the available TPA for PHA and TAG accumulation. The PHA yield was 0.011 ± 0.00 g_{PHA}/g_{TPA}, while a higher yield was reached for TAGs (0.031 ± 0.002 g_{TAG}/g_{TPA}). An overall consumption of 10.7 g/L of TPA was achieved over 28 h. Similar values

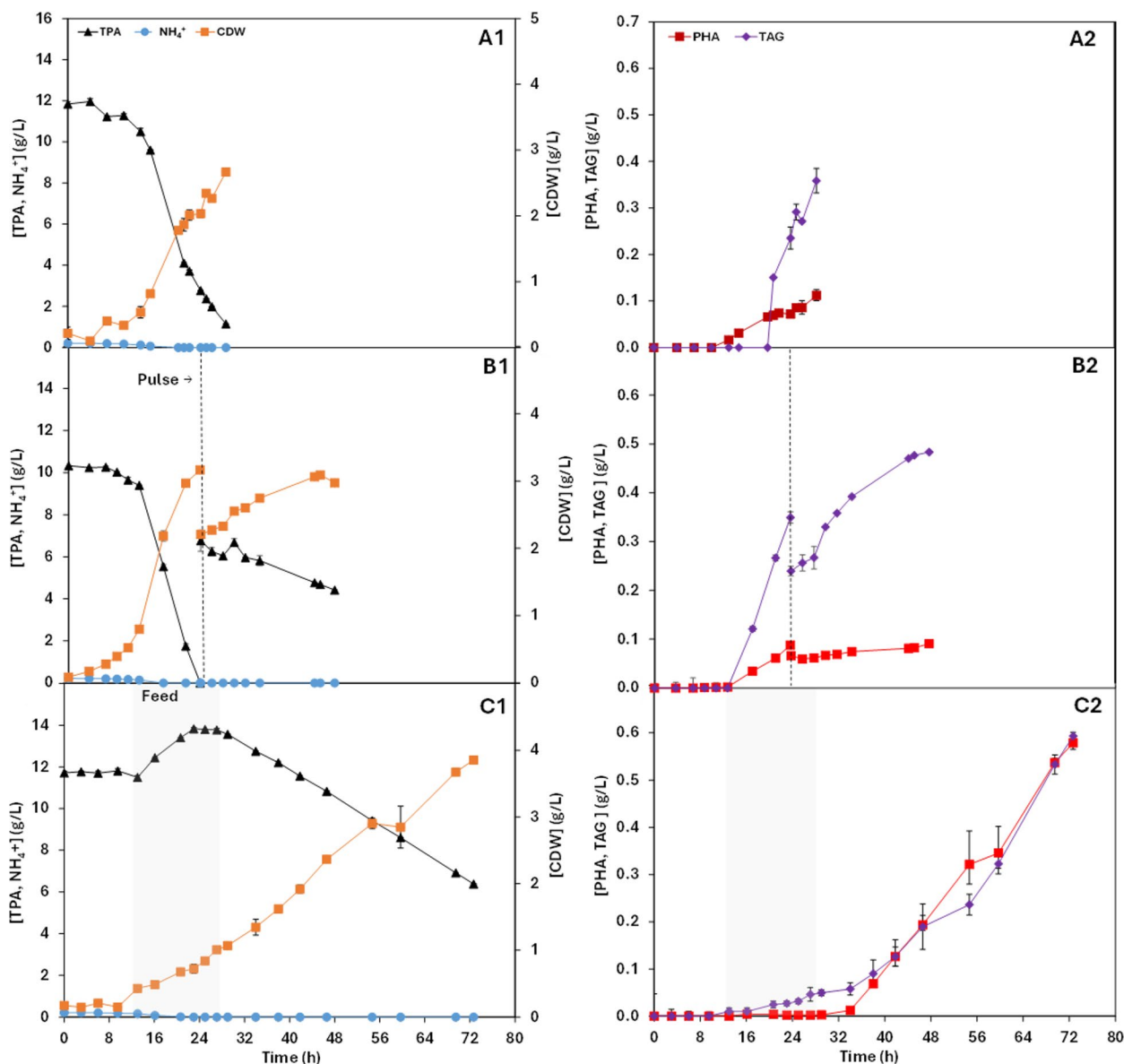


Fig. 4 Cultivation profiles for batch (A), fed-batch with pulse feed (the dashed line denotes the time the REX-TPA pulse was given) (B) and fed-batch with continuous feed (the grey area denotes the time REX-TPA was fed to the bioreactor, at a rate of 0.1 L/h) (C) of *Rhodococcus* sp. Ave7 using REX-TPA as feedstock. Error bars correspond to triplicate measurements

were obtained for *P. umsongensis* GO16 KS3 cultivated in TPA and EG obtained by enzymatic PET hydrolysis, ($0.21 \text{ g}_{\text{CDW}}/\text{g}_{\text{substrate}}$ and $0.014 \text{ g}_{\text{PHA}}/\text{g}_{\text{substrate}}$, respectively) [27].

Fed-batch cultivation with pulse feeding

In Assay B (Fig. 4(B1)), *Rhodococcus* sp. Ave7 entered the exponential growth phase after 9 h of cultivation, presenting a maximum specific growth rate of $0.18 \pm 0.02 \text{ h}^{-1}$, which was not significantly ($p > 0.05$) different from Assay A ($0.18 \pm 0.05 \text{ h}^{-1}$). Ammonia depletion was observed after 17 h of cultivation, resulting in a CDW

of $2.18 \pm 0.13 \text{ g/L}$. By 24 h, the culture achieved a maximum CDW of $3.17 \pm 0.03 \text{ g/L}$ (Fig. 4(B1)), with PHA and TAGs contents of $2.77 \pm 0.01 \text{ wt.}\%$ and $11.03 \pm 0.36 \text{ wt.}\%$, respectively. At this moment, dissolved oxygen concentration started to increase (data not shown), indicating depletion of the carbon source. Therefore, a 1 L REX-TPA pulse (containing 20 g/L TPA) was fed to the culture, rising the TPA concentration to $6.76 \pm 0.87 \text{ g/L}$.

During the first 24 h, *Rhodococcus* sp. Ave7 produced $0.09 \pm 0.00 \text{ g/L}$ of PHA (Fig. 4(B2)). Despite the subsequent feeding of a TPA pulse, no further increase in

Table 3 Kinetic and stoichiometric parameters of the three assays performed by *Rhodococcus* sp. Ave7 using REX-TPA

| Parameter | Cultivation | | | p value |
|--|---------------|---------------|---------------|---------|
| | A | B | C | |
| μ_{\max} (h ⁻¹) | 0.18 ± 0.05 | 0.18 ± 0.02 | 0.17 ± 0.01 | n.s. |
| CDW (g/L) | 2.67 ± 0.06 | 2.97 ± 0.05 | 3.85 ± 0.09 | *** |
| PHA (wt.%) | 4.22 ± 0.03 | 3.05 ± 0.05 | 15.01 ± 0.68 | *** |
| PHA (g/L) | 0.11 ± 0.02 | 0.09 ± 0.00 | 0.58 ± 0.02 | *** |
| TAG (wt.%) | 13.45 ± 0.69 | 16.26 ± 0.12 | 15.40 ± 0.29 | *** |
| TAG (g/L) | 0.36 ± 0.05 | 0.48 ± 0.04 | 0.59 ± 0.04 | ** |
| r_{PHA} (g/(L day)) | 0.096 ± 0.000 | 0.062 ± 0.000 | 0.245 ± 0.001 | *** |
| r_{TAG} (g/(L day)) | 0.305 ± 0.001 | 0.331 ± 0.001 | 0.252 ± 0.021 | *** |
| $Y_{\text{PHA/TPA}}$ (g _{PHA} /g _{TPA}) | 0.011 ± 0.00 | 0.015 ± 0.001 | 0.051 ± 0.003 | *** |
| $Y_{\text{TAG/TPA}}$ (g _{TAG} /g _{TPA}) | 0.031 ± 0.002 | 0.081 ± 0.001 | 0.052 ± 0.000 | *** |

μ_{\max} maximum specific cell growth, CDW cell dry weight, r_{PHA} PHA volumetric productivity, r_{TAG} TAG volumetric productivity, $Y_{\text{PHA/TPA}}$ PHA polymer yield on TPA basis, $Y_{\text{TAG/TPA}}$ TAG yield on TPA basis, n.s. not significant

$p > 0.05$; * $p \leq 0.05$; ** $p \leq 0.01$; *** $p \leq 0.001$

PHA concentration was observed until the end of the assay, resulting in a final polymer content in the cells of 3.05 ± 0.05 wt.%, a significant statistical decrease from the previous assay, corresponding to an overall volumetric productivity of 0.062 g/(L day) (Table 3). This PHA accumulation is comparable to that achieved by engineered *Pseudomonas stutzeri* TPA3P (3.66 wt.%) whilst using commercial bis(2-hydroxyethyl) TPA (BHET) as carbon source that yielded 3.54 g/L of biomass [28].

Regarding TAG accumulation, *Rhodococcus* sp. Ave7 achieved a biomass content of 11.03 wt.%, corresponding to a concentration of 0.35 ± 0.04 g/L (Fig. 4(B2)), within the first 24 h of cultivation. After the TPA pulse provided at 24 h, under ammonia-limited conditions, TAG content continued to increase, reaching 0.48 ± 0.04 g/L (Fig. 4(B2)) by the end of the cultivation. This represented a final TAG content in the biomass of 16.26 ± 0.12 wt.%, corresponding to an overall volumetric productivity of 0.331 g/(L day) (Table 3).

The TPA pulse conditions tested in Assay B resulted in a statistically significant increase in TAG content to 16.3 ± 0.1 wt.% compared to the value obtained in Assay A under batch mode (13.5 ± 0.7 wt.%) (Table 3). Previous studies with different *Rhodococcus* strains reported PHA and TAG accumulation capabilities. For instance, *Rhodococcus jostii* RHA1, when grown on glucose or gluconate, accumulated PHA contents ranging from 2 to 7.6 wt.% and TAGs content representing 56 wt.% of the CDW [51]. Moreover, *Rhodococcus aetherivorans* IAR1, grown on acetate or toluene, accumulated 10–12 wt.% PHA and 24 wt.% TAG of the CDW (Table 4) [40]. Although *Rhodococcus* sp. Ave7 did not reach comparable TAG

contents in this study, its PHA accumulation, using REX-TPA as the sole carbon source, was comparable to that of the reported strains.

The initial TPA (10.30 ± 0.01 g/L) available in the bioreactor was depleted within 24 h of cultivation, while further 2.34 g/L were consumed after the pulse, corresponding to an overall uptake of 12.67 ± 0.03 g/L. Moreover, a growth yield of 0.40 g_x/g_{TPA} was obtained, while the products' yields were 0.015 g_{PHA}/g_{TPA} and 0.081 g_{TAG}/g_{TPA} (Table 3).

Fed-batch cultivation with continuous feeding

Aiming to further enhance PHA and TAG accumulation, Assay C was conducted with continuous feeding that was initiated after 13 h of cultivation. The culture presented a lag phase of approximately 10 h (Fig. 4(C1)), similar to those observed in Assays A and B. Afterwards, the bacterium entered an exponential phase with a maximum cell growth rate of 0.17 ± 0.01 h⁻¹ (Table 3). TPA consumption remained low during the lag phase of the cultivation (0.22 g/L). At the start of the exponential phase, a continuous REX-TPA feed was initiated at a rate of 0.1 L/h, which lasted 15 h. As shown in Fig. 4(C1), TPA concentration in the bioreactor increased between 13 and 21 h, reaching 13.8 g/L of TPA, which coincided with the onset of cell growth in the cultivation.

By the end of the experiment (73 h), the culture reached a maximum CDW of 3.58 ± 0.09 g/L (Table 3), which was significantly higher ($p \leq 0.001$) than the values obtained in assay A and B. TAG production started around 13 h (Fig. 4(C1)), representing 15.40 ± 0.29 wt.% of the CDW, with a final concentration of 0.59 ± 0.04 g/L (Fig. 4(C2)), corresponding to a volumetric productivity of 0.252 ± 0.021 g/(L day) (Table 3). These values are slightly lower than those obtained in Assay A and B (0.305 ± 0.001 g/L and 0.331 ± 0.001 g/(L day), respectively).

Interestingly, PHA synthesis was initiated around the same time of TAG, but it continued until the end of the assay, reaching a polymer content of 15.01 ± 0.68 wt.% (0.58 g/L) (Fig. 4(C2)). PHA concentration was significantly higher than that observed for Assays A and B, leading to an overall volumetric productivity of 0.245 ± 0.001 g/(L day) (Table 3). These results are close to those reported and patented for *Rhodococcus pyridinivorans* P23, a bacterium isolated from a PET film, which achieved similar levels of PHA accumulation when cultivated with commercial TPA (15 wt.%) or disodium terephthalate (23.8 wt.%) (Table 4) as substrates [42]. Moreover, *R. aetherivorans* IAR1, grown under batch mode using acetate or in fed-batch mode with toluene as sole carbon sources, displayed a similar production profile to the one obtained in this experiment and

Table 4 Assessment of PHA, TAG and bioproducts from PET degradation products and pollutants feedstocks from various microbial source

| Microbial source | Substrate | Cultivation mode | Time (h) | Biomass (g/L) | PHA (wt. %) | TAG (wt. %) | Bioproducts | Reference | | |
|--|---|----------------------|----------|---|-------------|---------------|--------------------------|------------|---------|--|
| <i>Rhodococcus</i> sp. Ave7 | REX-TPA | Bioreactor | 28–73 | 2.67–3.85 | 3.05–15.0 | 13.45–16.26 | PHBV TAG | This study | | |
| <i>Rhodococcus pyridinivorans</i> P23 | TPA | Erlenmeyer | 24–96 | 2.14 | 15 | n.a | PHBV | [42] | | |
| | Disodium terephthalate | | | 2.65 | 23.8 | n.a | | | | |
| <i>Priesta</i> sp. | REX-TPA | Shake Flask | n.a | 1.06 | 4.14 | n.a | PHA | [65] | | |
| <i>Streptomyces</i> sp. | | | n.a | 1.39 | 0.32 | n.a | | | | |
| <i>Pseudomonas umsongensis</i> GO16 KS3 | Hydrolyzed PET | Bioreactor | 28 | 2.3 | 7 | n.a | mcl-PHA HAAs | [27] | | |
| Engineered <i>Pseudomonas putida</i> AW165 | BHET | Bioreactor | 96 | n.a | n.a | n.a | β -ketoadipic acid | [32] | | |
| Engineered <i>Pseudomonas stutzeri</i> TPA3P | BHET | Erlenmeyer | 54 | 3.54 | 3.66 | n.a | PHB | [28] | | |
| <i>Pseudomonas umsongensis</i> GO16 | Sodium terephthalate | Shake Flask | 48 | 3.5 | 27 | n.a | mcl-PHA | [26] | | |
| | | | | <i>Pseudomonas putida</i> GO19 | 3.5 | 23 | n.a | | | |
| <i>Pseudomonas frederiksbergensis</i> GO23 | | | | 4 | 14 | n.a | | | | |
| <i>Pseudomonas umsongensis</i> GO16 | Sodium terephthalate | Fed-batch Bioreactor | 48 | 8.7 | 30 | n.a | mcl-PHA | [25] | | |
| | | | | Sodium terephthalate supplemented with waste glycerol | 48 | 14.3 | 36 | n.a | mcl-PHA | |
| | | | | 15.1 | 35 | n.a | | | | |
| | | | | 14.1 | 35 | n.a | | | | |
| | | | | 11.7 | 36 | n.a | | | | |
| <i>Pseudomonas putida</i> F1 | Benzene Toluene Ethylbenzene | Shake flask | 48 | 0.34 | 22 | n.a | mcl-PHA | [66] | | |
| | | | | 0.72 | 15 | n.a | | | | |
| | | | | 0.67 | 14 | n.a | | | | |
| <i>Pseudomonas putida</i> MT-2 | Toluene Xylene | Shake flask | 48 | 0.37 | 22 | n.a | | | | |
| | | | | 0.53 | 26 | n.a | | | | |
| Consortium of <i>Pseudomonas putida</i> (F1 + mt-2 + CA-3) | BTEXS mixture | Batch Bioreactor | 48 | 1.03 | 24 | n.a | | | | |
| <i>Rhodococcus aetherivorans</i> IAR1 | Toluene | Erlenmeyer | 80 | 2.5 | 10 | 24 | PHBV TAG | [40] | | |
| <i>Rhodococcus jostii</i> RHA 1 | Hexadecane | Erlenmeyer | n.a | n.a | Tr | 30.4 | PHBV TAG | [51] | | |
| | Hexadecane + Hexadecanol | | n.a | n.a | Tr | 7.0 | | | | |
| <i>Rhodococcus</i> sp. A5 | Hexadecane | Erlenmeyer | 48 | n.a | Tr | 1.3–1.9 32 | PHA TAG | [67] | | |
| <i>Rhodococcus opacus</i> PD630 | Petroleum wastewater supplemented with molasses | Bioreactor | 96 | 5.91 | n.a | 52.5 | Lipids | [68] | | |
| | | | | 7.24 | n.a | 54.4 | | | | |
| <i>Rhodococcus</i> sp. 602 | n-hexadecane | Erlenmeyer | 48 | n.a | n.a | 22.3 | PHA TAG | [69] | | |
| | Benzoate | | | n.a | 8.2 | 64.9 | | | | |

EG ethylene glycol, HAAs hydroxyalkanoxy-alkanoates monomers, BHET commercial bis(2-hydroxyethyl) TPA, BTEXS benzene, toluene, ethylbenzene, p-xylene, PHBV poly(3-hydroxybutyrate-co-3-hydroxyvalerate); n.a. not available, tr traces

synthesizing simultaneously both products during bacterial exponential phase. However, a lower PHA accumulation was reached (between 10 and 12 wt.%) (Table 4) [40].

Nonetheless, the results showed that under the conditions of assays A and B, TAG accumulation (13.45 and 16.30 wt.%) was favoured over PHA synthesis (4.22 and 3.05 wt.%). On the other hand, in assay C, under continuous feeding, after ammonia depletion and with higher TPA availability, the TAG content remained comparable (15.40 wt.%) to assay B, while PHA accumulation showed a statically significant increase (from 3.05 to 15 wt.%) ($p \leq 0.001$). These findings suggest that higher TPA availability during continuous feeding of the carbon source apparently enhanced the flux towards PHA synthesis in *Rhodococcus* sp. Ave7, when ammonia became limiting.

In assay C, under continuous feeding conditions, a total of approximately 16.5 g/L of TPA were consumed, surpassing the consumption observed in Assay B. This resulted in growth yield of 0.24 g_X/g_{TPA} , along with products' yields of 0.051 g_{PHA}/g_{TPA} and 0.052 g_{TAG}/g_{TPA} for PHA and TAG (Table 3), respectively, demonstrating significant improvement ($p \leq 0.001$) when compared to Assays A and B. Statistical analysis (Table S2, Supplementary Material) confirmed that continuous feeding significantly enhanced PHA accumulation compared to pulse feeding, while TAG accumulation remained statistically similar between Assays B and C. These findings underscore the metabolic flexibility of *Rhodococcus* sp. Ave7 under different feeding strategies and reinforce its potential for biotechnological applications.

Additionally, the yields obtained in Assay C are higher than those reported for *P. umsongensis* GO16 KS3 (0.21 $g_{CDW}/g_{substrate}$ and 0.014 $g_{PHA}/g_{substrate}$), although this study was carried out in batch reactor [27].

According to several literature reports, some *Rhodococcus* strains can accumulate intracellular reserves of glycogen or PolyP [70]. However, no glycogen nor PolyP were detected for *Rhodococcus* sp. Ave7 in any of the assays.

Overall, the bioreactor assays demonstrated that *Rhodococcus* sp. Ave7 possesses a high capacity for TPA degradation, consuming 30.46 ± 0.25 g in 73 h while yielding two value-added bio-products. Biomass concentrations up to 3.85 g/L were reached, which is higher than the values reported, for example, for *R. pyridinivorans* P23 (2.14–2.65 g/L) and *P. umsongensis* G016 KS3 (2.3 g/L), grown on similar feedstocks, including TPA and TPA derived from PET depolymerization (Table 4) [27, 42].

Additionally, *Rhodococcus* sp. Ave7 was able to accumulate PHA and TAGs as the main intracellular products, conducted under REX-TPA excess and an ammonia-limiting strategy. The values obtained for PHA accumulation with *Rhodococcus* sp. Ave7 are in accordance with those reported in literature for other bacteria

tested on PET degradation products. Microorganism from different genera have been reported to utilize REX-TPA as substrate; however, these cultivations were conducted under shake flask conditions, with strains such as *Priestia* sp. and *Streptomyces* sp. yielding polymer content of 4.14 wt.% and 0.32%, respectively (Table 4) [65].

The PHA content in *Rhodococcus* sp. Ave7 biomass in assay C was significantly higher than the values reported for other *Rhodococcus* species. For instance, for *R. jostii* RHA1 grown on a mixture hexadecane and hexadecanol, only traces of PHA were detected [51]. Similarly, *Rhodococcus* sp. 602, which was grown on benzoate, accumulated 8.2 wt.% of PHA [69]. On the other hand, TAG production by *Rhodococcus* sp. Ave7 reached values similar to those reported by *R. jostii* when using mixtures of hexadecane and hexadecanol (7.0%) [51]. However, it was lower than the 54.4% produced by *R. opacus* PD630 grown on petroleum wastewater supplemented with molasses (Table 4) [68].

Limitations of productivity

This study is the first to describe the use of synthetic PET residue (REX-TPA) as a feedstock for producing TAGs and PHAs, offering potential findings for PET waste recycling and plastic upcycling. However, several challenges remain, particularly in terms of yield and productivity of both bioproducts. The volumetric productivities of PHA (0.245 g/(L day)) and TAG (0.252 g/(L day)) under continuous feeding conditions are relatively low compared to reported standards, 1.6–4.6 g/(L h) and 0.21 g/(L h) for PHA and TAGs, respectively [71–73]. This presents a significant hurdle for the economic feasibility of large-scale applications.

Rhodococcus sp. Ave7 exhibited a long lag phase, a common challenge reported for TPA-degrading bacteria [74] and an isolated *Rhodococcus biphenylivorans* strain [75]. Optimizing inoculum preparation such as using a pre-inoculum, supplementing with a secondary carbon source [25], or adapting the culture to the feedstock by gradually increasing REX-TPA concentrations over multiple generations, could enhance growth rates, as demonstrated in *P. umsongensis* GO16 for EG degradation [27].

Despite achieving a CDW of 3.85 g/L, comparable to other strains utilizing plastic-derived feedstocks, biomass concentration remains insufficient for industrial application. This limitation is partly due to the poor solubility of TPA free acid in aqueous media (approximately 0.017 g/L at 25 °C) [25]. While conversion to sodium terephthalate improves solubility (~130 g/L) [76], it requires large REX-TPA feed volumes to reach comparable concentrations of other substrates [25]. Thus, supplementing a more readily metabolizable co-substrate could help mitigate this issue that impacts biomass concentration and

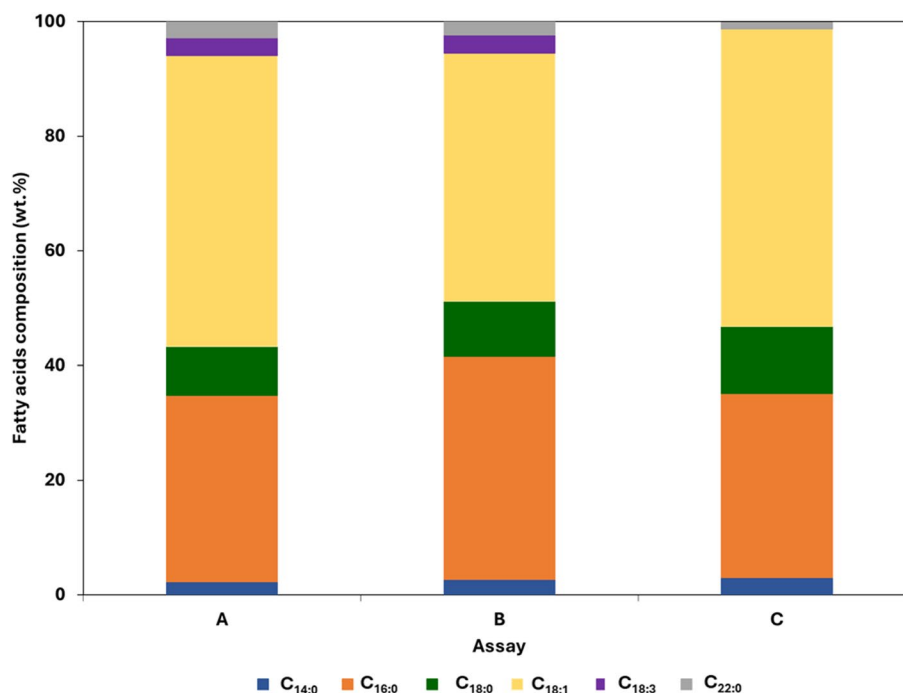


Fig. 5 Fatty acids composition of the TAGs produced by *Rhodococcus sp. Ave7* attained in biomass obtained at the end of the cultivation assays

product productivity. For example, *P. umsongensis* GO16 showed enhanced growth (from 8.7 to 15.1 g/L) (Table 4) when tested in fed-batch bioreactor with PET pyrolysis-derived TPA and waste glycerol supplementation [25]. Similarly, *R. opacus* PD630 cultivated in petroleum wastewater with molasses supplementation achieved biomass concentrations of 5.91 to 7.24 g/L (Table 4) [68]. High-cell density cultivation, as employed for *R. opacus* PD630 producing TAGs from lignocellulosic feedstocks [73], may also be a viable approach.

Since fed-batch cultivation enhanced both bioproduct and biomass production in *Rhodococcus sp. Ave7*, it would be particularly interesting to determine the optimal impact of REX-TPA feeding strategies. Employing sodium terephthalate could limit biomass growth due to potential inhibition from sodium accumulation associated with non-growth consumption, as previously reported for *P. umsongensis* GO16 [77].

Furthermore, *Rhodococcus sp. Ave7* conversion efficiency of TPA to desired products remained low, with PHA and TAG yields of 0.051 g_{PHA}/g_{TPA} and 0.052 g_{TAG}/g_{TPA}, respectively. This suggests that a significant portion of the substrate is being diverted away from PHA and TAG biosynthesis. Metabolic engineering strategies could be explored to enhance carbon flux toward bioproduct formation, potentially improving yields and productivities [78].

Addressing these limitations is crucial for developing a more efficient and scalable bioprocess, advancing this technology towards industrial application.

Characterization of intracellular storage compounds Composition

Cis-9-octadecenoic acid (C_{18:1}) (43.3–50.8 wt.%) and hexadecanoic acid (C_{16:0}) (32.1–38.9 wt.%) were the predominant fatty acids in the TAG produced in all assays, with lower contents of octadecanoic acid (C_{18:0}) (8.5–8.7 wt.%) (Fig. 5). Moreover, in assays A and B, 3.1–3.2 wt.% of *cis,cis,cis*-9,12,15-octadecatrienic acid (C_{18:3}), a polyunsaturated fatty acid was also detected, together with other minor fatty acids fractions, such as tetradecanoic acid (C_{14:0}) (2.3–3.0 wt.%) and docosanoic acid (C_{22:0}) (1.2–2.9 wt.%).

Similar fatty acids compositions were detected for *R. pyridinivorans* CCZU-B16 and *R. aetherivorans* IAR1, although their relative contents were significantly different. *R. pyridinivorans* CCZU-B16 TAG presented a fatty acids profile rich in C_{16:0} (22.4%), C_{16:1} (21.1%), C_{18:0} (16.2%) and C_{18:1} (23.1%) [79]. Furthermore, *R. aetherivorans* IAR1 was also reported as TAGs producer from toluene, showing a profile in fatty acids mainly comprising C_{16:0} (~50%), followed by C_{18:1} (25%), with fatty acids such as C_{18:0}, C_{17:0}, C_{16:1} and C_{14:0} also being detected [40]. *Rhodococcus sp. Ave7* cultivated in REX-TPA represents a source of TAGs rich in fatty acids, comparable to

Table 5 Monomeric composition of PHA from *Rhodococcus* sp. Ave7 biomass at the end of cultivation assays

| Assay | PHA composition (wt.%) | |
|-------|------------------------|------------|
| | 3 HB | 3 HV |
| A | 39.5 ± 0.2 | 60.5 ± 0.2 |
| B | 11.9 ± 0.3 | 88.1 ± 0.3 |
| C | 8 ± 0.1 | 92.0 ± 0.1 |

n.d. not detected, 3HB 3-hydroxybutyrate, 3HV 3-hydroxyvalerate

the species *R. rhodochrous*, which produced TAG composed mostly of C_{16:0} (35%) and C_{18:1} (42%) [80].

The predominance of C_{18:1} and C_{16:0} fatty acids, commonly found in soybean oil and palm oil, renders *Rhodococcus* sp. Ave7 TAG as potential candidates, for example, for biodiesel as oxidative stabilizer, cetane number and balancing cold flow [80]. These findings suggest the possibility of using the produced fatty acids as a complementary and renewable source alongside these oils, whilst valorising a PET waste through a more sustainable approach [81].

Regarding the PHA produced by *Rhodococcus* sp. Ave7, in all assays, a co-polymer of 3-hydroxybutyrate (3HB) and 3-hydroxyvalerate (3HV) monomers, namely PHBV, was obtained. As shown in Table 5, 3HV is the main monomer in all assays, accounting for 60.5 ± 0.2 wt.% of the biopolymer produced in Assay A under batch conditions, while under fed-batch mode, it increased, representing 88.1 ± 0.3 wt.% and 92.0 ± 0.1 wt.% in Assays B and C, respectively (Table 5).

Similar composition, namely high 3HV contents, was reported for PHBV synthesized by different *Rhodococcus* sp. For instance, *R. ruber* NCIM 40126 grown on different substrates, such as acetate, fructose, glucose, presented 3HV as the main monomer, at contents ranging from 69 to 84 mol%, whilst *R. rhodochrous* ATCC19070 reached 3HV contents between 73 and 97 mol% while using the same substrate [82]. Additionally, *R. aetherivorans* IAR23 produced a PHA with 79 mol% of 3HV and 21 mol% of 3HB on acetate, increasing the 3HV fraction to 80 mol% when grown on toluene [40, 83]. *R. pyridinivorans* P23 is reported to synthesize PHA with 3HV monomer content higher than 60 mol% using TPA as feedstock [42].

This study demonstrated that REX-TPA can be used as feedstock for the synthesis of high 3HV content PHBV by *Rhodococcus* sp. Ave7. This increased proportion in 3HV in the polyester presents the opportunity for tuning properties such as thermal features, which are crucial for the manipulation during processing of PHBV copolymer blends applications [84]. It has been reported, for copolymers with 3HV contents similar to the one obtained in this study, melting temperatures (89–110 °C) in the range of those reported for PHBV 50–80 mol% with a variation

regarding the crystallinity degree (54–62%), which affects directly on the biodegradability of the material [84, 85]. Furthermore, the production of PHBV is highly priced when compared to fossil-fuel-derived plastics [86]; therefore, exploiting *Rhodococcus* sp. Ave7 upcycling of TPA from depolymerized non-recyclable PET waste establishes the opportunity to render a more environmental and circular economic process for plastics.

FTIR

The FT-IR spectra for TAGs produced in assay C (Fig. 6(a)) show a band around 2853 and 2922 cm⁻¹ are related to the asymmetric and symmetric stretching vibrations of the C-H bonds in the alkane hydrocarbon chains of fatty acids in TAGs [87]. The intense peak at 1744 cm⁻¹ is related to C=O stretching vibration in ester groups of TAGs [88]. Moreover, a weaker peak at 1654 cm⁻¹ associated with C=C stretching vibrations was detected, indicating the presence of unsaturated bonds in C_{18:1} structure, one of the main fatty acids that compose TAGs produced by *Rhodococcus* sp. Ave7 [89]. Additionally, the bands observed between 1098 and 1158 cm⁻¹ correspond to the stretching vibration of C-O bond in TAGs ester groups. The band at 1464 cm⁻¹ is related with the deforming vibration of C-H bonds in aliphatic groups of TAGs [88]. A band at 722 cm⁻¹ appears due to the vibration of the -CH₂ groups present in C_{18:1} structure [87].

When compared to the FT-IR spectra of a soybean oil (Fig. 6(b)), a relevant reference due to its similar composition to the TAGs produced by *Rhodococcus* sp. Ave7, particularly the presence of C_{18:1}, C_{18:0} and C_{16:0} fatty acids, both spectra share similar features, such as the intense 1743 cm⁻¹ peak for C=O stretching and the 2922 and 2853 cm⁻¹ peaks for C-H vibrations, indicating a comparable TAG structure. However, variations in peak intensity or position, such as those observed for the 1159 cm⁻¹ band in soybean oil, reflect differences in the composition of unsaturated fatty acids and potential variations in the degree of saturation or chain length of fatty acids [91]. These differences likely result from the distinct cultivation conditions of *Rhodococcus* sp. Ave7 and TAGs recovery methods used.

The FT-IR spectra (Fig. 7(a)) for PHBV produced by *Rhodococcus* sp. Ave7 shows an intense peak at 1723 cm⁻¹, corresponding to the stretching band of the carbonyl group (-C=O) [92], characteristic of PHA spectra. Peaks between 2855 and 2964 cm⁻¹ are associated with the C-H stretching vibrations of the methyl and the methylene groups in the polymer structure and side chain [92], while the broad region between 969 and 1074 cm⁻¹ corresponds to the C-C bonds [93]. The peak at 1258 cm⁻¹, linked to the asymmetric stretching of

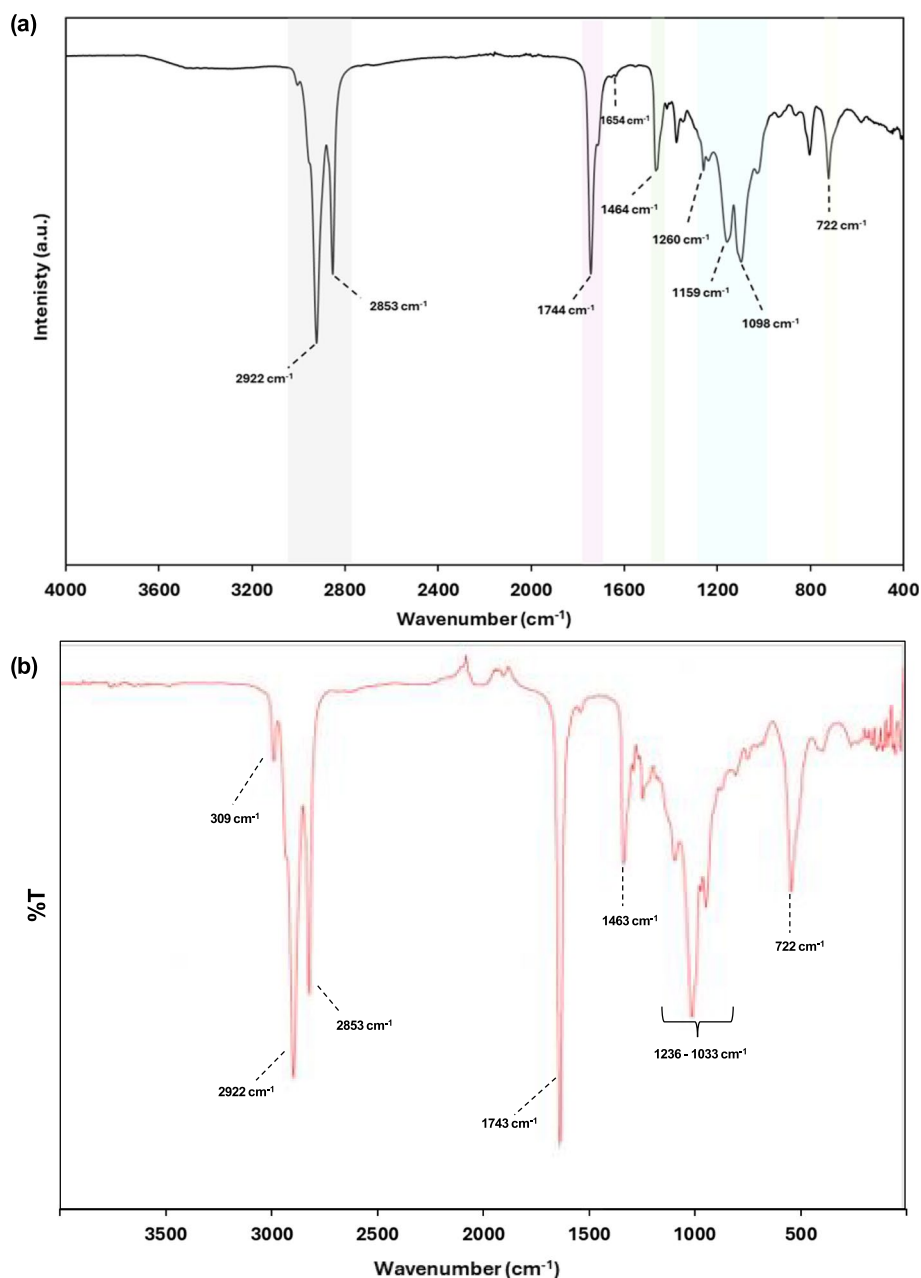


Fig. 6 FT-IR spectra for (a) TAGs produced by *Rhodococcus* sp. Ave7 during fed-batch with continuous feed conditions and (b) soybean oil (adapted from [90])

saturated ester bond (C–O–C) [92], is associated with the crystallinity of the biopolymer, suggesting that low crystallinity is expected for the PHBV produced by *Rhodococcus* sp. Ave7 [53]. In comparison to the PHBV with 11% 3HV content (Fig. 7(b)), the spectra for PHBV produced by *Rhodococcus* sp. Ave7 (Fig. 7(a)) exhibits notable differences, particularly in the intensity of this peak further suggesting the reduced crystallinity of the polymer attained by *Rhodococcus*. Additionally, the variations

in the band at 1452 cm^{-1} , associated with CH_2 bending vibrations, highlight the influence of compositional differences in the polymer backbone.

Molecular mass distribution

The PHBV produced had a molecular weight (M_w) of 277 kDa and a polydispersity index (PDI) of 1.5 (Table 6), falling within the typical range of M_w (250–820 kDa) and PDI (1.4 to 2.7) values reported for PHBV with high 3HV

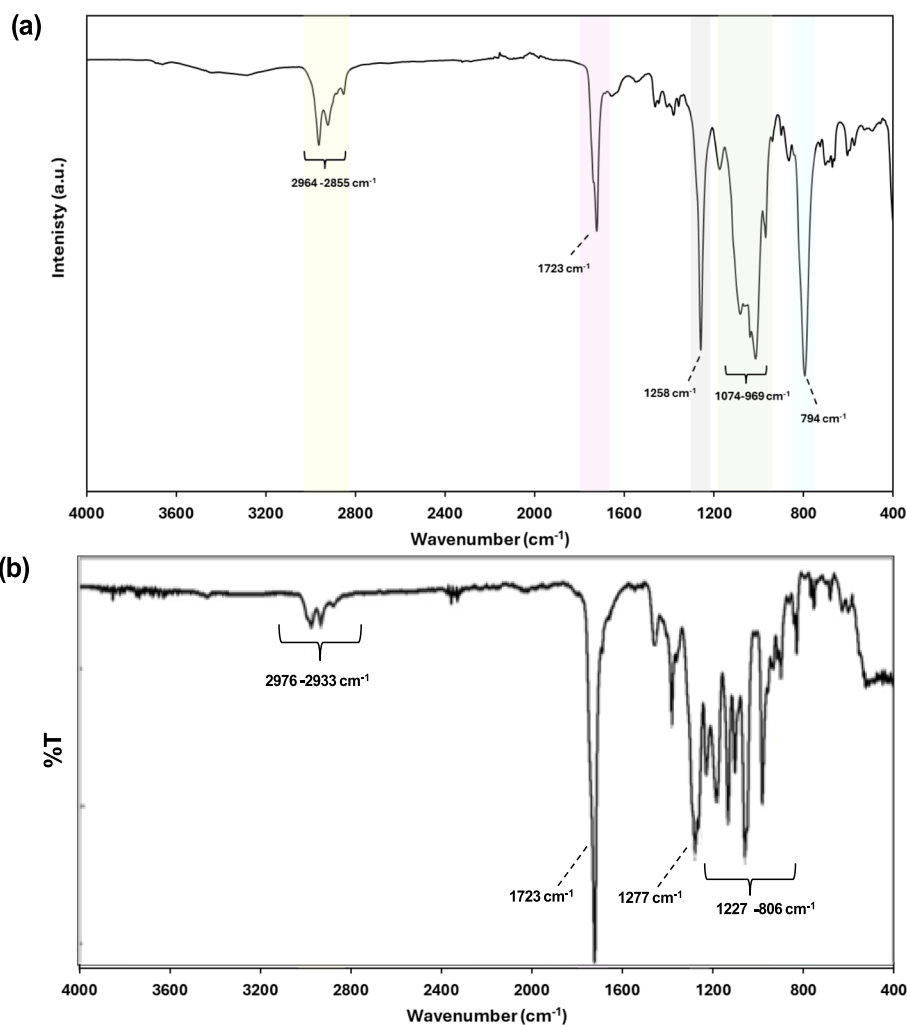


Fig. 7 FT-IR spectra for (a) PHBV produced by *Rhodococcus* sp. Ave7 during fed-batch with continuous feed conditions and (b) PHBV with 11% 3HV content (adapted from [94])

Table 6 Physical- chemical and thermal properties of PHBV produced in Assay C from *Rhodococcus* sp. Ave7

| Characterization | Value |
|-----------------------|-------|
| Mw (kDa) | 277 |
| PDI | 1.5 |
| T _m (°C) | 95.1 |
| ΔH _m (J/g) | 26.3 |
| X _c (%) | 18.0 |
| T _g (°C) | -21.1 |
| T _{deg} (°C) | 270.0 |
| | 395.5 |
| | 503.6 |

Mw molecular weight, PDI polydispersity index, T_m melting temperature, T_g glass transition temperature, T_{deg} degradation temperature, ΔH_m melting enthalpy, X_c crystallinity fraction

content (58 to 98 mol%) [85]. Moreover, the M_w and PDI obtained was also comparable to the PHBV, 260 kDa and PDI of 1.9, produced by mixed microbial cultures with 82 mol% 3HV [84]. Nevertheless, the M_w attained for *Rhodococcus* sp. Ave7 PHBV was low compared to the produced by *R. pyridinivorans* P23 (M_w of 600 kDa) using TPA, but still within the same order of magnitude [42].

The PDI of the PHBV attained in assay C suggests a good polymer uniformity, which may facilitate its processing and biodegradation rate [95, 96].

Thermal properties

The biopolymer presented a melting temperature (T_m) of 95.1 °C that is within the range of several PHBV with 3HV contents varying between 58 and 98 mol% (89.9–109.4 °C) [85], and similar to the T_m (101 °C) reported for PHBV produced with TPA as feedstock [42]. The high

3HV content in the copolymer lowers the T_m significantly, thus broadening its processability window, which facilitates the polymer processing in comparison to the homopolymer composed by 3HB, characterized by a T_m very close to the degradation temperature [97].

The PHBV also exhibited a glass transition temperature (T_g) of $-21.1\text{ }^\circ\text{C}$ (Table 6), which is significantly lower than the typical values reported for PHBV with 3HV contents of 82 mol% ($-13.2\text{ }^\circ\text{C}$) [84]. The low T_g observed for PHBV may result from TAGs still present in the polymer matrix after 1-butanol precipitation, potentially acting as plasticizers that increase the free volume between PHBV chains and enhance their mobility at lower temperatures, as reported for PHBV and plasticizers blends [89, 98].

The polymer presented a crystallinity of 18.0% (Table 6), indicating it was more amorphous than other 3HV-rich PHBV (40–50 mol % of 3HV) that present crystallinities within 50% [85]. For copolymers where 3HV content was higher, a higher crystallinity was expected since it would mainly take the crystal structure of the P(3HV) homopolymer lattice [99]. This decrease in crystallinity may be related to the presence of remnants of TAGs that were not completely removed from the sample [100], as previously detected in the biopolymer FT-IR spectrum. Nevertheless, the biopolymer's low crystallinity may provide more flexibility compared to other PHBV blends with lower 3HV content, making it suitable for applications that require softer, more flexible materials [84].

The biopolymer was thermally stable until $270\text{ }^\circ\text{C}$ (Table 6), in concomitant with degradation temperature (T_{deg}) ($279\text{ }^\circ\text{C}$) for other 3HV-rich PHBV, where it suffered a weight loss of 46% [101]. Above this temperature, a second weight loss of 15.5% was attained at $395.5\text{ }^\circ\text{C}$ followed by a third observed at $503.6\text{ }^\circ\text{C}$ for 33.8% of weight loss. These later stages of degradation are attributed to the degradation of fatty acids, confirming the decomposition of TAGs monounsaturated and saturated fatty acids, mainly composed by $C_{18:1}$, $C_{16:0}$ and $C_{18:0}$ [102].

The presence of fatty acids significantly affected the thermal properties of the sample. The fatty acids within the polymer matrix exhibited higher T_{deg} than the individual oleic, stearic and palmitic methyl esters ($210\text{--}229\text{ }^\circ\text{C}$ for 5% weight loss) or their ethylene glycol esters ($228\text{--}248\text{ }^\circ\text{C}$) tested as potential PHBV plasticizers [89]. This shows that the presence of TAGs-derived fatty acids in the polymer provide a higher window of thermal stability compared to previously PHBV composites with similar fatty acids. This demonstrates that PHBV materials with high 3HV content can be tailored by adding natural fatty acids as plasticizers, enhancing the biopolymer's performance, particularly in the thermal stability for end-use applications [89].

Conclusions

This work validated *Rhodococcus* sp. Ave7 as a promising microorganism for the bioremediation of PET waste, given its high capacity for TPA bioconversion. The culture efficiently upcycled depolymerized PET waste into biomass, PHA and TAGs. The produced co-polyester PHBV, with a 3HV content up to 90 wt.%, has potential for being used in PHBV copolymer blends. The biosynthesized TAGs, on the other hand, were enriched in octadecenoic and hexadecanoic acids, which might be of interest to pair with the existing production from vegetable oils sources. Overall, this study demonstrated the potential of *Rhodococcus* sp. Ave7 for effective biodegradation of chemically depolymerized PET waste into value-added bio-based products, thus contributing to reduce the impact of PET waste and valorising it into value-added products, within the circular economy concept. Through the bioconversion of PET waste into sustainable alternatives to petroleum-derived plastics and oils, this research supports efforts to reduce plastic waste and dependence on fossil-based resources, underlining its role in advancing sustainable waste management solutions and reinforcing its environmental and societal relevance.

Abbreviations

| | |
|------------|--|
| PET | Polyethylene terephthalate |
| TPA | Terephthalic acid |
| REX | Reactive extrusion |
| REX-TPA | Reactive extrusion-terephthalic acid |
| PHAs | Polyhydroxyalkanoates |
| TAGs | Triacylglycerols |
| PHBV | Poly(3-hydroxybutyrate-co-3-hydroxyvalerate) |
| 3HV | 3-Hydroxyvalerate |
| $C_{18:1}$ | Octadecenoic acid |
| $C_{16:0}$ | Hexadecanoic acid |

Supplementary Information

The online version contains supplementary material available at <https://doi.org/10.1186/s44314-025-00019-4>.

Supplementary Material 1. Table S1 Matrix of the Response Surface Methodology (RSM), composed of eleven experiments: four factorial design points; four experiments of axial level; and a central point with three replicas. The two independent variable, X_1 (REX-TPA concentration, g/L) and X_2 (Ammonium concentration, g/L) and the response Y_1 (CDW, g/L), Y_2 (PHA wt.%) and Y_3 (TAG, wt.%) for *Rhodococcus* sp. Ave7. Table S2 One-way ANOVA results for kinetic and stoichiometric parameters of the three assays performed by *Rhodococcus* sp. Ave7 using REX-TPA. Fig. S1 Three-dimensional response surface and contour plots show the interactive effects of different concentrations of ammonium and REX-TPA on CDW (g/L) (a), PHA (wt.%) (b) and TAG (wt.%) (c) for *Rhodococcus* sp. Ave7.

Acknowledgements

Not applicable.

Authors' contributions

Conceptualization: ATR, CT, and FF; formal analysis: ATR, CT and FF; investigation: ATR; methodology: ATR; HK, LS, OA; writing—original draft: ATR; writing—review and editing: MF, CT, CET, MM, MR and FF. All authors have read and agreed to the published version of the manuscript.

Funding

This work was financed by the European Union's Horizon 2020 research and innovation program through Project Bio Innovation of a Circular Economy for Plastics (BioICEP), under grant agreement No. 870292, supported by the National Natural Science Foundation of China (grant numbers: Institute of Microbiology, Chinese Academy of Sciences: 31961133016; Beijing Institute of Technology: 31961133015; Shandong University: 31961133014). European Union's Horizon Europe EIC Pathfinder programme, Eco conversion of lower grade PET and mixed recalcitrant PET plastic waste into high performing biopolymers (EcoPlastic), under grant agreement No 101046758. By national funds from FCT—Fundação para a Ciência e a Tecnologia, I.P., in the scope of the projects UIDP/04378/2020 and UIDB/04378/2020 of the Research Unit on Applied Molecular Biosciences—UCIBIO and the project LA/P/0140/2020 of the Associate Laboratory Institute for Health and Bioeconomy—i4HB. A.T.R. acknowledges FCT I.P. for the Ph.D. grant 2020.06470.BD.

Data availability

No datasets were generated or analysed during the current study.

Declarations

Ethics approval consent to participate

Not applicable.

Consent for publication

Not applicable.

Competing interests

The authors declare no competing interests.

Received: 8 July 2024 Accepted: 3 March 2025

Published online: 25 March 2025

References

- Nisticò R. Polyethylene terephthalate (PET) in the packaging industry. *Polym Test*. 2020;90: 106707. <https://doi.org/10.1016/j.polymertesting.2020.106707>.
- Maurya A, Bhattacharya A, Khare SK. Enzymatic remediation of polyethylene terephthalate (PET)-based polymers for effective management of plastic wastes: an overview. *Front Bioeng Biotechnol*. 2020;8: 602325. <https://doi.org/10.3389/fbioe.2020.602325>.
- Samak NA, Jia Y, Sharshar MM, Mu T, Yang M, Peh S, et al. Recent advances in biocatalysts engineering for polyethylene terephthalate plastic waste green recycling. *Environ Int*. 2020;145: 106144. <https://doi.org/10.1016/j.envint.2020.106144>.
- Thomsen TB, Almdal K, Meyer AS. Significance of poly(ethylene terephthalate) (PET) substrate crystallinity on enzymatic degradation. *New Biotechnol*. 2023;78:162–72. <https://doi.org/10.1016/j.nbt.2023.11.001>.
- Kim NK, Lee SH, Park HD. Current biotechnologies on depolymerization of polyethylene terephthalate (PET) and repolymerization of reclaimed monomers from PET for bio-upcycling: A critical review. *Bioresour Technol*. 2022;363: 127931. <https://doi.org/10.1016/j.biortech.2022.127931>.
- Soong YHV, Sobkowicz MJ, Xie D. Recent advances in biological recycling of polyethylene terephthalate (PET) Plastic Wastes. *Bioengineering*. 2022;9(3):98. <https://doi.org/10.3390/bioengineering9030098>.
- Pereira EHDS, Attallah OA, Tas CE, Chee BS, Freitas F, Garcia EL, et al. Boosting bacterial nanocellulose production from chemically recycled post-consumer polyethylene terephthalate. *Sustain Mater Technol*. 2024;39: e00784. <https://doi.org/10.1016/j.susmat.2023.e00784>.
- Verma R, Vinoda KS, Papireddy M, Gowda ANS. Toxic pollutants from plastic waste—a review. *Procedia Environ Sci*. 2016;35:701–8. <https://doi.org/10.1016/j.proenv.2016.07.069>.
- Barredo A, Asueta A, Amundarain I, Leivar J, Miguel-Fernández R, Arnaiz S, et al. Chemical recycling of monolayer PET tray waste by alkaline hydrolysis. *J Environ Chem Eng*. 2023;11(3): 109823. <https://doi.org/10.1016/j.jece.2023.109823>.
- Singh N, Hui D, Singh R, Ahuja IPS, Feo L, Fraternali F. Recycling of plastic solid waste: A state of art review and future applications. *Compos B Eng*. 2017;115:409–22. <https://doi.org/10.1016/j.compositesb.2016.09.013>.
- Grigore ME. Methods of recycling, properties and applications of recycled thermoplastic polymers. *Recycling*. 2017;2(4):1–11. <https://doi.org/10.3390/recycling2040024>.
- Faust K, Denifl P, Hapke M. Recent advances in catalytic chemical recycling of polyolefins. *Chem Cat Chem*. 2023;15(13): e202300310. <https://doi.org/10.1002/cctc.202300310>.
- Jabłońska B. Water consumption management in polyethylene terephthalate (PET) bottles washing process via wastewater pretreatment and reuse. *J Environ Manage*. 2018;224:215–24. <https://doi.org/10.1016/j.jenvman.2018.07.054>.
- Thachnatharen N, Shahabuddin S, Sridewi N. The waste management of polyethylene terephthalate (PET) plastic waste: a review. *IOP Conf Ser Mater Sci Eng*. 2021;1127(1): 012002. <https://doi.org/10.1088/1757-899X/1127/1/012002>.
- Damayanti, Wu HS. Strategic possibility routes of recycled pet. *Polymers*. 2021; 13(9):1475. <https://doi.org/10.3390/polym13091475>.
- Soni VK, Singh G, Vijayan BK, Chopra A, Kapur GS, Ramakumar SSV. Thermochemical recycling of waste plastics by pyrolysis: a review. *Energy Fuels*. 2021;35(16):12763–808. <https://doi.org/10.1021/acs.energyfuels.1c01292>.
- Cao F, Wang L, Zheng R, Guo L, Chen Y, Qian X. Research and progress of chemical depolymerization of waste PET and high-value application of its depolymerization products. *RSC Adv*. 2022;12(49):31564–76. <https://doi.org/10.1039/D2RA06499E>.
- Muñoz Meneses RA, Cabrera-Papamija G, Machuca-Martínez F, Rodríguez LA, Diosa JE, Mosquera-Vargas E. Plastic recycling and their use as raw material for the synthesis of carbonaceous materials. *Heliyon*. 2022;8(3): e09028. <https://doi.org/10.1016/j.heliyon.2022.e09028>.
- Al-Salem SM, Lettieri P, Baeyens J. Recycling and recovery routes of plastic solid waste (PSW): A review. *Waste Manage*. 2009;29(10):2625–43. <https://doi.org/10.1016/j.wasman.2009.06.004>.
- Lomwongsopon P, Varrone C. Critical review on the progress of plastic bioupcycling technology as a potential solution for sustainable plastic waste management. *Polymers*. 2022;14(22):4996. <https://doi.org/10.3390/polym14224996>.
- Mudondo J, Lee HS, Jeong Y, Kim TH, Kim S, Sung BH, et al. Recent advances in the chemobiological upcycling of polyethylene terephthalate (PET) into value-added chemicals. *J Microbiol Biotech*. 2023;33(1):1–14. <https://doi.org/10.4014/jmb.2208.08048>.
- Kalathil S, Miller M, Reisner E. Microbial Fermentation of Polyethylene Terephthalate (PET) Plastic waste for the production of chemicals or electricity. *ChemRxiv*. 2022;61(45): e202211057. <https://doi.org/10.1002/anie.202211057>.
- Ru J, Huo Y, Yang Y. Microbial degradation and valorization of plastic wastes. *Front Microbiol*. 2020;11:442. <https://doi.org/10.3389/fmicb.2020.00442>.
- Fujiwara R, Sanuki R, Ajiro H, Fukui T, Yoshida S. Direct fermentative conversion of poly(ethylene terephthalate) into poly(hydroxyalkanoate) by *Ideonella sakaiensis*. *Sci Rep*. 2021;11(1). <https://doi.org/10.1038/s41598-021-99528-x>.
- Kenny ST, Runic JN, Kaminsky W, Woods T, Babu RP, O'Connor KE. Development of a bioprocess to convert PET derived terephthalic acid and biodiesel derived glycerol to medium chain length polyhydroxyalkanoate. *Appl Microbiol Biotechnol*. 2012;95(3):623–33. <https://doi.org/10.1007/s00253-012-4058-4>.
- Kenny ST, Runic JN, Kaminsky W, Woods T, Babu RP, Keely CM, et al. Upcycling of PET (Polyethylene Terephthalate) to the biodegradable plastic PHA (Polyhydroxyalkanoate). *Environ Sci Technol*. 2008;42(20):7696–701. <https://doi.org/10.1021/es801010e>.
- Tiso T, Narancic T, Wei R, Pollet E, Beagan N, Schröder K, et al. Towards bio-upcycling of polyethylene terephthalate. *Metab Eng*. 2021;66:167–78. <https://doi.org/10.1016/j.jmben.2021.03.011>.
- Liu P, Zhang T, Zheng Y, Li Q, Su T, Qi Q. Potential one-step strategy for PET degradation and PHB biosynthesis through co-cultivation of two engineered microorganisms. *Engineering Microbiology*. 2021;1: 100003. <https://doi.org/10.1016/j.engmic.2021.100003>.

29. Esmail A, Rebocho AT, Marques AC, Silvestre S, Gonçalves A, Fortunato E, et al. Bioconversion of terephthalic acid and ethylene glycol into bacterial cellulose by *Komagataeibacter xylinus* DSM 2004 and DSM 46604. *Front Bioeng Biotechnol*. 2022;10: 853322. <https://doi.org/10.3389/fbioe.2022.853322>.
30. Liu P, Zheng Y, Yuan Y, Zhang T, Li Q, Liang Q, et al. Valorization of polyethylene terephthalate to muconic acid by engineering *Pseudomonas Putida*. *Int J Mol Sci*. 2022;23(19):10997. <https://doi.org/10.3390/ijms231910997>.
31. Sadler JC, Wallace S. Microbial synthesis of vanillin from waste poly(ethylene terephthalate). *Green Chem*. 2021;23(13):4665–72. <https://doi.org/10.1039/D1GC00931A>.
32. Werner AZ, Clare R, Mand TD, Pardo I, Ramirez KJ, Haugen SJ, et al. Tandem chemical deconstruction and biological upcycling of poly(ethylene terephthalate) to β -keto adipic acid by *Pseudomonas putida* KT2440. *Metab Eng*. 2021;67:250–61. <https://doi.org/10.1016/j.ymben.2021.07.005>.
33. Gao R, Pan H, Kai L, Han K, Lian J. Microbial degradation and valorization of poly(ethylene terephthalate) (PET) monomers. *World J Microb Biot*. 2022;38(5):89. <https://doi.org/10.1007/s11274-022-03270-z>.
34. Kim HT, Kim JK, Cha HG, Kang MJ, Lee HS, Khang TU, et al. Biological valorization of poly(ethylene terephthalate) monomers for upcycling waste PET. *ACS Sustain Chem Eng*. 2019;7(24):19396–406. <https://doi.org/10.1021/acssuschemeng.9b03908>.
35. Cappelletti M, Presentato A, Piacenza E, Firrincieli A, Turner RJ, Zannoni D. Biotechnology of *Rhodococcus* for the production of valuable compounds. *Appl Microbiol Biot*. 2020;104:8567–94. <https://doi.org/10.1007/s00253-020-10861-z>.
36. Ivshina I, Bazhutin G, Tyumina E. *Rhodococcus* strains as a good biotool for neutralizing pharmaceutical pollutants and obtaining therapeutically valuable products: Through the past into the future. *Front Microbiol*. 2022;13:1–28. <https://doi.org/10.3389/fmicb.2022.967127>.
37. Hara H, Eltis LD, Davies JE, Mohn WW. Transcriptomic analysis reveals a bifurcated terephthalate degradation pathway in *Rhodococcus* sp. strain RHA1. *J Bacteriol*. 2007;189(5):1641–7. <https://doi.org/10.1128/jb.01322-06>.
38. Kumar V, Maitra SS, Singh R, Burnwal DK. Acclimatization of a newly isolated bacteria in monomer tere-phthalic acid (TPA) may enable it to attack the polymer poly-ethylene tere-phthalate(PET). *J Environ Chem Eng*. 2020;8(4): 103977. <https://doi.org/10.1016/j.jece.2020.103977>.
39. Kim D, Choi KY, Yoo M, Zylstra GJ, Kim E. Biotechnological potential of *Rhodococcus* biodegradative pathways. *J Microbiol Biotech*. 2018;28(7):1037–51. <https://doi.org/10.4014/jmb.1712.12017>.
40. Hori K, Abe M, Unno H. Production of triacylglycerol and poly(3-hydroxybutyrate-co-3-hydroxyvalerate) by the toluene-degrading bacterium *Rhodococcus aetherivorans* IAR1. *J Biosci Bioeng*. 2009;108(4):319–24. <https://doi.org/10.1016/j.jbiosc.2009.04.020>.
41. Maurya AC, Bhattacharya A, Khare SK. Biodegradation of terephthalic acid using *Rhodococcus erythropolis* MTCC 3951: Insights into the degradation process, applications in wastewater treatment and polyhydroxy-alkanoate production. *Environ Sci Pollut R*. 2024;31:57376–85. <https://doi.org/10.1007/s11356-023-30054-1>.
42. Guo W, Shao Z. *Rhodococcus pyridinivorans* and application thereof in production of PHBV. CN112063567A. 2020.
43. Altaee N, El-Hiti GA, Fahdil A, Sudesh K, Yousif E. Screening and evaluation of poly(3-hydroxybutyrate) with *Rhodococcus equi* using different carbon sources. *Arab J Sci Eng*. 2017;42(6):2371–9. <https://doi.org/10.1007/s13369-016-2327-8>.
44. Alvarez HM, Steinbüchel A. Triacylglycerols in prokaryotic microorganisms. *Appl Microbiol Biotechnol*. 2002;60(4):367–76. <https://doi.org/10.1007/s00253-002-1135-0>.
45. Castro AR, Rocha I, Alves MM, Pereira MA. *Rhodococcus opacus* B4: a promising bacterium for production of biofuels and biobased chemicals. *AMB Express*. 2016;6(1):35. <https://doi.org/10.1186/s13568-016-0207-y>.
46. Tao X, Ouyang H, Zhou A, Wang D, Matlock H, Morgan JS, et al. Polyethylene degradation by a *Rhodococcus* strain isolated from naturally weathered plastic waste enrichment. *Environ Sci Technol*. 2023;57(37):13901–11. <https://doi.org/10.1021/acs.est.3c03778>.
47. Krivoruchko A, Kuyukina M, Ivshina I. Advanced *Rhodococcus* biocatalysts for environmental biotechnologies. *Catalysts*. 2019;9(3):23–30. <https://doi.org/10.3390/catal9030236>.
48. Fournet MB, Attallah OA, Mojicevic M, Chen Y, Major I. High throughput mechanochemical depolymerisation and purification of polyethylene terephthalate and related polymers. WO2023088946A1. 2022.
49. Yang X. Rapid determination of eight related aromatic acids in the p-phthalic acid mother liquid using an Agilent 1260 Infinity LC system and an Agilent Poroshell 120 SB-C18 column [Application Note]. Shanghai (China): Agilent Technologies Co. Ltd; 2013.
50. Lanham AB, Ricardo AR, Coma M, Fradinho J, Carvalheira M, Oehmen A, et al. Optimisation of glycogen quantification in mixed microbial cultures. *Bioresour Technol*. 2012;118:518–25. <https://doi.org/10.1016/j.biortech.2012.05.087>.
51. Hernández MA, Mohn WW, Martínez E, Rost E, Alvarez AF, Alvarez HM. Biosynthesis of storage compounds by *Rhodococcus jostii* RHA1 and global identification of genes involved in their metabolism. *BMC Genomics*. 2008;9:600. <https://doi.org/10.1186/1471-2164-9-600>.
52. Rebocho AT, Pereira JR, Neves LA, Alves VD, Sevrin C, Grandfils C, et al. Preparation and characterization of films based on a natural p(3hb)/mcl-pha blend obtained through the co-culture of cupriavidus necator and pseudomonas citronellolis in apple pulp waste. *Bioengineering*. 2020;7(2):34. <https://doi.org/10.3390/bioengineering7020034>.
53. Esmail A, Pereira R, Sevrin C, Grandfils C, Menda UD, Fortunato E, et al. Preparation and characterization of porous scaffolds based on poly(3-hydroxybutyrate) and poly(3-hydroxybutyrate-co-3-hydroxyvalerate). *Life*. 2021;11(9):935. <https://doi.org/10.3390/life11090935>.
54. Abdesoltan H. A focused review on recycling and hydrolysis techniques of polyethylene terephthalate. *Polym Eng Sci*. 2023;63(9):2651–74. <https://doi.org/10.1002/pen.26406>.
55. Azeem M, Fournet MB, Attallah OA. Ultrafast 99% Polyethylene terephthalate depolymerization into value added monomers using sequential glycolysis-hydrolysis under microwave irradiation. *Arab J Chem*. 2022;15(7): 103903. <https://doi.org/10.1016/j.arabjc.2022.103903>.
56. Wang Y, Zhang Y, Song H, Wang Y, Deng T, Hou X. Zinc-catalyzed ester bond cleavage: Chemical degradation of polyethylene terephthalate. *J Clean Prod*. 2019Jan;20(208):1469–75. <https://doi.org/10.1016/j.jclepro.2018.10.117>.
57. Liu Y, Yao X, Yao H, Zhou Q, Xin J, Lu X, et al. Degradation of poly(ethylene terephthalate) catalyzed by metal-free choline-based ionic liquids. *Green Chem*. 2020;22(10):3122–31. <https://doi.org/10.1039/D0GC00327A>.
58. Štrukil V. Highly efficient solid-state hydrolysis of waste polyethylene terephthalate by mechanochemical milling and vapor-assisted aging. *Chemoschem*. 2021;14(1):330–8. <https://doi.org/10.1002/cssc.202002124>.
59. Wang Y, Kretschmer K, Zhang J, Mondal AK, Guo X, Wang G. Organic sodium terephthalate@graphene hybrid anode materials for sodium-ion batteries. *RSC Adv*. 2016;6(62):57098–102. <https://doi.org/10.1039/c6ra11809g>.
60. Deng Q, Wang Y, Zhao Y, Li J. Disodium terephthalate/multiwall-carbon nanotube nanocomposite as advanced anode material for Li-ion batteries. *Ionics*. 2017;23(10):2613–9. <https://doi.org/10.1007/s11581-016-1951-3>.
61. Lee HL, Chiu CW, Lee T. Engineering terephthalic acid product from recycling of PET bottles waste for downstream operations. *Chemical Engineering Journal Advances*. 2021;5: 100079. <https://doi.org/10.1016/j.cej.2020.100079>.
62. Amundarain I, Asueta A, Leivar J. Optimization of pressurized alkaline hydrolysis for chemical recycling of post-consumer PET waste. *Materials*. 2024;17(11):2619. <https://doi.org/10.3390/ma17112619>.
63. Sinha V, Patel MR, Patel JV. Pet waste management by chemical recycling: a review. *J Polym Environ*. 2010;18(1):8–25. <https://doi.org/10.1007/s10924-008-0106-7>.
64. Klöckner P, Reemtsma T, Wagner S. The diverse metal composition of plastic items and its implications. *Sci Total Environ*. 2021;764: 142870. <https://doi.org/10.1016/j.scitotenv.2020.142870>.
65. Herrera DAG, Mojicevic M, Pantelic B, Joshi A, Collins C, Batista M, et al. Exploring microorganisms from plastic-polluted sites: unveiling plastic degradation and PHA production potential. *Microorganisms*. 2023;11(12):2914. <https://doi.org/10.3390/microorganisms11122914>.

66. Nikodinovic J, Kenny ST, Babu RP, Woods T, Blau WJ, O'Connor KE. The conversion of BTEX compounds by single and defined mixed cultures to medium-chain-length polyhydroxyalkanoate. *Appl Microbiol Biotechnol.* 2008;80(4):665–73. <https://doi.org/10.1007/s00253-008-1593-0>.
67. Bequer Urbano S, Albarracín VH, Ordoñez OF, Fariás ME, Alvarez HM. Lipid storage in high-altitude Andean Lakes extremophiles and its mobilization under stress conditions in *Rhodococcus* sp. A5, a UV-resistant actinobacterium. *Extremophiles.* 2013;17(2):217–27. <https://doi.org/10.1007/s00792-012-0508-2>
68. Saisriyoot M, Sahaya T, Thanapimmetha A, Chisti Y, Srinophakun P. Production of potential fuel oils by *Rhodococcus opacus* grown on petroleum processing wastewaters. *J Renew Sustain Energy.* 2016;8(6):063106. <https://doi.org/10.1063/1.4971875>.
69. Silva RA, Grossi V, Olivera NL, Alvarez HM. Characterization of indigenously *Rhodococcus* sp. 602, a strain able to accumulate triacylglycerides from naphthyl compounds under nitrogen-starved conditions. *Res Microbiol.* 2010;161(3):198–207. <https://doi.org/10.1016/j.resmic.2010.01.007>
70. Tajparast M, Frigon D. Genome-scale metabolic model of *Rhodococcus jostii* RHA1 (iMT1174) to study the accumulation of storage compounds during nitrogen-limited condition. *BMC Syst Biol.* 2015;9(1):43. <https://doi.org/10.1186/s12918-015-0190-y>.
71. Blunt W, Levin DB, Cicek N. Bioreactor operating strategies for improved polyhydroxyalkanoate (PHA) productivity. *Polymers.* 2018;10(11). <https://doi.org/10.3390/polym10111197>
72. J. Brigham C, Kurosawa K. bacterial carbon storage to value added products. *J Microb Biochem Technol.* 2011;S3:002. <https://doi.org/10.4172/1948-5948.S3-002>
73. Kurosawa K, Boccazzi P, de Almeida NM, Sinskey AJ. High-cell-density batch fermentation of *Rhodococcus opacus* PD630 using a high glucose concentration for triacylglycerol production. *J Biotechnol.* 2010;147(3–4):212–8. <https://doi.org/10.1016/j.jbiotec.2010.04.003>.
74. Yastrebova OV, Malysheva AA, Plotnikova EG. Halotolerant terephthalic acid-degrading bacteria of the genus *Glutamicibacter*. *Appl Biochem Microbiol.* 2022;58(5):590–7. <https://doi.org/10.1134/S0003683822050167>.
75. Suwanawat N, Parakulsuksatid P, Nitayapat N, Sanpamongkolchai W. Biodegradation of terephthalic acid by *Rhodococcus biphenylivorans* isolated from soil. *Int J Environ Sci Dev.* 2019;10(1):30–3. <https://doi.org/10.18178/ijesd.2019.10.1.1141>
76. Müller C, Heck CA, Stephan L, Paschetag M, Scholl S. Precipitation of terephthalic acid from alkaline solution: influence of temperature and precipitation acid. *Ind Eng Chem Res.* 2023;62(30):12029–40. <https://doi.org/10.1021/acs.iecr.2c04451>.
77. Beagan N, O'Connor KE, Del Val JJ. Model-based operational optimisation of a microbial bioprocess converting terephthalic acid to biomass. *Biochem Eng J.* 2020;158: 107576. <https://doi.org/10.1016/j.bej.2020.107576>.
78. Manoli MT, Gargantilla-Becerra Á, del Cerro Sánchez C, Rivero-Buceta V, Prieto MA, Nogales J. A model-driven approach to upcycling recalcitrant feedstocks in *Pseudomonas putida* by decoupling PHA production from nutrient limitation. *Cell Rep.* 2024;43(4). <https://doi.org/10.1016/j.celrep.2024.113979>
79. Chong GG, Huang XJ, Di JH, Xu DZ, He YC, Pei YN, et al. Biodegradation of alkali lignin by a newly isolated *Rhodococcus pyridinivorans* CCZU-B16. *Bioproc Biosyst Eng.* 2018;41(4):501–10. <https://doi.org/10.1007/s00449-017-1884-x>.
80. Shields-Menard SA, Amirsadeghi M, Sukhbaatar B, Revellame E, Hernandez R, Donaldson JR, et al. Lipid accumulation by *Rhodococcus rhodochromus* grown on glucose. *J Ind Microbiol Biotechnol.* 2015;42(5):693–9. <https://doi.org/10.1007/s10295-014-1564-7>.
81. Ahmad FB, Zhang Z, Doherty WOS, O'Hara IM. The prospect of microbial oil production and applications from oil palm biomass. *Biochem Eng J.* 2019;143:9–23. <https://doi.org/10.1016/j.bej.2018.12.003>.
82. Haywoodt GW, Anderson AJ, Williams DR, Dawes EA, Ewing DF. Accumulation of a poly (hydroxyalkanoate) copolymer containing primarily 3-hydroxyvalerate from simple carbohydrate substrates by *Rhodococcus* sp. NCIMB 40126. *Int J Biol Macromol.* 1991;13(2):83–8. [https://doi.org/10.1016/0141-8130\(91\)90053-W](https://doi.org/10.1016/0141-8130(91)90053-W)
83. Hori K, Kobayashi A, Ikeda H, Unno H. *Rhodococcus aetherivorans* IAR1, a new bacterial strain synthesizing poly(3-hydroxybutyrate-co-3-hydroxyvalerate) from toluene. *J Biosci.* 2009;107(2):145–50. <https://doi.org/10.1016/j.jbiosc.2008.10.005>.
84. Langford A, Chan CM, Pratt S, Garvey CJ, Laycock B. The morphology of crystallisation of PHBV/PHBV copolymer blends. *Eur Polym J.* 2019;112:104–19. <https://doi.org/10.1016/j.eurpolymj.2018.12.022>.
85. Feng L, Wang Y, Inagawa Y, Kasuya K, Saito T, Doi Y, et al. Enzymatic degradation behavior of comonomer compositionally fractionated bacterial poly(3-hydroxybutyrate-co-3-hydroxyvalerate)s by poly(3-hydroxyalkanoate) depolymerases isolated from *Ralstonia pickettii* T1 and *Acidovorax* sp. TP4. *Polym Degrad Stab.* 2004;84(1):95–104. <https://doi.org/10.1016/j.polymdegradstab.2003.09.016>
86. Policastro G, Panico A, Fabbriano M. Improving biological production of poly(3-hydroxybutyrate-co-3-hydroxyvalerate) (PHBV) co-polymer: a critical review. *Rev Environ Sci Biotechnol.* 2021;20(2):479–513. <https://doi.org/10.1007/s11157-021-09575-z>.
87. Chaturvedi D, Bharti D, Dhal S, Sahu D, Behera H, Sahoo M, et al. Role of stearic acid as the crystal habit modifier in Candelilla wax-groundnut oil oleogels. *ChemEngineering.* 2023;7(5):96. <https://doi.org/10.3390/chemengineering7050096>.
88. Suri K, Singh B, Kaur A, Singh N. Impact of roasting and extraction methods on chemical properties, oxidative stability and Maillard reaction products of peanut oils. *J Food Sci Technol.* 2019;56(5):2436–45. <https://doi.org/10.1007/s13197-019-03719-4>.
89. Nosal H, Moser K, Warzala M, Holzer A, Stańczyk D, Sabura E. Selected fatty acids esters as potential phb-v bioplasticizers: effect on mechanical properties of the polymer. *J Polym Environ.* 2020;29(1):38–53. <https://doi.org/10.1007/s10924-020-01841-5>.
90. Vahur S, Teearu A, Peets P, Joosu L, Leito I. Database of ATR-FT-IR spectra of various materials. ATR-FT-IR spectrum of fresh soybean oil (4000–225 cm⁻¹). University of Tartu. <https://spectra.chem.ut.ee/paint/binders/soybean-oil/>. Accessed 12 Jan 2025.
91. Poiana MA, Alexa E, Munteanu MF, Gligor R, Moigradean D, Mateescu C. Use of ATR-FTIR spectroscopy to detect the changes in extra virgin olive oil by adulteration with soybean oil and high temperature heat treatment. *Open Chem.* 2015;13(1):689–98. <https://doi.org/10.1515/chem-2015-0110>.
92. Ponjavic M, Malagurski I, Lazic J, Jeremic S, Pavlovic V, Prlainovic N, et al. Advancing PHBV Biomedical Potential with the Incorporation of Bacterial Biopigment Prodigiosin. *Int J Mol Sci.* 2023;24(3):1906. <https://doi.org/10.3390/ijms24031906>.
93. Ajmal AW, Masood F, Yasin T. Influence of sepiolite on thermal, mechanical and biodegradation properties of poly-3-hydroxybutyrate-co-3-hydroxyvalerate nanocomposites. *Appl Clay Sci.* 2018;156:11–9. <https://doi.org/10.1016/j.clay.2018.01.010>.
94. Chaber P, Tylko G, Włodarczyk J, Nitschke P, Hercog A, Jurczyk S, et al. Surface modification of phbv fibrous scaffold via lithium borohydride reduction. *Materials.* 2022;15(21):7494. <https://doi.org/10.3390/ma15217494>.
95. Elhami V, van de Beek N, Wang L, Picken SJ, Tamis J, Sousa JAB, et al. Extraction of low molecular weight polyhydroxyalkanoates from mixed microbial cultures using bio-based solvents. *Sep Purif Technol.* 2022;299: 121773. <https://doi.org/10.1016/j.seppur.2022.121773>.
96. Hong SG, Hsu HW, Ye MT. Thermal properties and applications of low molecular weight polyhydroxybutyrate. *J Therm Anal Calorim.* 2013;111(2):1243–50. <https://doi.org/10.1007/s10973-012-2503-3>.
97. Urtuvia V, Ponce B, Andler R, Diaz-barrera A. Relation of 3HV fraction and thermomechanical properties of poly(3-hydroxybutyrate-co-3-hydroxyvalerate) produced by *Azotobacter vinelandii* OP. *Int J Biol Macromol.* 2023;253(8): 127681. <https://doi.org/10.1016/j.jbiomac.2023.127681>.
98. Umamura RT, Felisberti MI. Plasticization of poly(3-hydroxybutyrate) with triethyl citrate: Thermal and mechanical properties, morphology, and kinetics of crystallization. *J Appl Polym Sci.* 2021;138(10):1–14. <https://doi.org/10.1002/app.49990>.
99. Wang Y, Yamada S, Asakawa N, Yamane T, Yoshie N, Inoue Y. Comonomer compositional distribution and thermal and morphological characteristics of bacterial poly(3-hydroxybutyrate-co-3-hydroxyvalerate)s with high 3-hydroxyvalerate content. *Biomacromol.* 2001;2(4):1315–23. <https://doi.org/10.1021/bm010128o>.
100. Kaniuk Ł, Podborska A, Stachewicz U. Enhanced mechanical performance and wettability of PHBV fiber blends with evening primrose oil

- for skin patches improving hydration and comfort. *J Mater Chem B*. 2022;10(11):1763–74. <https://doi.org/10.1039/d1tb02805g>.
101. Chan CM, Vandi LJ, Pratt S, Halley P, Ma Y, Chen GQ, et al. Understanding the effect of copolymer content on the processability and mechanical properties of polyhydroxyalkanoate (PHA)/wood composites. *Compos Part A Appl Sci Manuf*. 2019;124: 105437. <https://doi.org/10.1016/j.compositesa.2019.05.005>.
 102. Sanahuja AB, Teruel NG, Carratalá MLM, Selva MCG. Characterization of almond cultivars by the use of thermal analysis techniques. Application to cultivar authenticity. *J Am Oil Chem Soc, Journal of the American Oil Chemists' Society*. 2011;88(11):1687–93. <https://doi.org/10.1007/s11746-011-1847-3>

Publisher's Note

Springer Nature remains neutral with regard to jurisdictional claims in published maps and institutional affiliations.